Title

The euphausiid prey field for blue whales around a steep bathymetric feature in the southern California current system

Journal

Limnology and Oceanography, 64(1)

ISSN

0024-3590

Authors

Nickels, Catherine F
Sala, Linsey M
Ohman, Mark D

Publication Date

2019

DOI

10.1002/lno.11047

Peer reviewed

LIMNOLOGY
and
OCEANOGRAPHY

ASLO

Limnol. Oceanogr. 9999, , 1–16

doi: 10.1002/lno.11047

The euphausiid prey field for blue whales around a steep bathymetric feature in the southern California current system

Catherine F. Nickels,* Linsey M. Sala, Mark D. Ohman
Scripps Institution of Oceanography, University of California San Diego, La Jolla, California

Abstract

Euphausiids are important prey for many marine organisms and often occur in patchy aggregations. Euphausiid predators, such as blue whales, may become concentrated in the vicinity of these aggregations. We investigated an area called Nine Mile Bank (NMB) near San Diego, California, defined by an area of steep bathymetry, to determine whether the frequent whale sightings in that locality can be explained by the distribution of euphausiids across the bank and by the vertical distribution of euphausiids in the water column. *Thysanoessa spinifera*, the strongly preferred blue whale prey euphausiid in this area, was consistently more abundant on the bank or inshore of it than offshore. In contrast, *Euphausia pacifica,* a minor blue whale prey item, was much more abundant and distributed across the study region. Adults of both species were concentrated in a stratum corresponding to the feeding depth of blue whales. Other euphausiids that form a negligible part of the blue whale diet also showed no association with NMB. Both blue whales and their primary prey species *Thysanoessa spinifera* were more abundant on or inshore of the bank than offshore, suggesting that the bank may serve as an offshore limit of high prey abundance that helps to concentrate blue whales.

Blue whales migrate into the southern sector of the California current system (CCS) to feed in summer and return to lower latitudes during the winter months (Burtenshaw et al. 2004; McDonald et al. 2006; Bailey et al. 2009). The density of blue whales is maximal in summer and decreases in fall, but blue whales are rare or absent from the southern CCS in winter and spring (Campbell et al. 2015). Blue whales are typically obligate predators on euphausiids (Schoenherr 1991; Croll et al. 2005; Nickels et al. 2018). In the central California region, blue whales feed mostly on *Thysanoessa spinifera* and to a much lesser extent *Euphausia pacifica,* to a lower size limit of approximately 10 mm (Croll et al. 1998). A similar strong dietary preference of blue whales for larger *T. spinifera* has recently been documented in the southern California region (Nickels et al. 2018). The whales' restricted choice of prey items limits the food resources available to blue whales and may serve to structure whale distributions.

In the southern sector of the CCS, blue whales appear from whale watching data to be sighted more frequently above steep bathymetric features than nearby (Bissell 2013), although whale watching data report only positive records and can be further biased by recurrent trips to the same sites. The association of whales with abrupt bathymetry has, however, also been reported in other locations. Blue whales sighted in Monterey Bay between 1992 and 1996 were concentrated along the edge of the Monterey submarine canyon (Croll et al. 2005). In 1995 and 1996, Fiedler et al. (1998) found abundant blue whales to the north of San Miguel and Santa Rosa Islands in the Channel Islands. North Atlantic blue whales forage along the slope of the Laurentian Channel, the continental shelf edge, some shelf habitats, and may utilize the New England Seamount chain (Lesage et al. 2017).

A likely explanation for this association with bathymetric features is increased productivity or aggregation of prey around abrupt features. In the St. Lawrence Estuary, Cotte and Simard (2005) found euphausiids aggregated by the interaction of sloped bathymetry, semidiurnal tidal currents, and euphausiid negative-phototactic swimming behavior. Euphausiid aggregation where upwelling takes place along sloping topography may help maintain them in regions with high potential productivity (Cotte and Simard 2005). Potential mechanisms for the formation of zooplankton aggregations around abrupt topography are reviewed by Genin (2004) and include upwelling-related increased productivity, bathymetric blockage of zooplankton descent, behavioral depth retention by swimming against upwelling water flow, and enhanced horizontal flux. While euphausiid aggregations can be displaced from regions of strong upwelling due to offshore advection, bathymetric features may alter this dynamic and

*Correspondence: cnickels@ucsd.edu

Additional Supporting Information may be found in the online version of this article.

retain euphausiids in areas of strong upwelling and productivity (Santora et al. 2011; Dorman et al. 2015).

Blue whales lunge feed, a behavior where food is captured in discrete events instead of continuous filtration (Kawamura 1980; Goldbogen et al. 2012; Goldbogen et al. 2017). Lunge feeding can occur at the surface or at depth and has been detected in eastern North Pacific blue whales only during the day (Calambokidis et al. 2007). Lunge feeding baleen whales require exceptionally high prey densities to offset their high energetic costs (Goldbogen et al. 2011), far above the average densities measured over large spatial scales (Croll et al. 2005). Hence, while both would be important to consider, local densities indicated by degree of patchiness may be more relevant than overall abundance in assessing the availability of prey to blue whales (Benoit-Bird et al. 2013). Patterns of patchiness can vary by both life history stage and species of euphausiid (Décima et al. 2010).

The abundances and distributions of blue whales and euphausiids are affected by climatic cycles and can vary interannually. The level of blue whale calling off of southern California during the 1998 El Niño was much lower than normal during their typical peak in mid-September, indicating either lower presence or a change in behavior of increased foraging activity, but the level of calling returned to normal during the 1999 La Niña (Burtenshaw et al. 2004). In summer 2014, the CCS experienced the effects of strong warm anomalies in the Northeast Pacific (Leising et al. 2015). Euphausiid abundance during the 2014 warm event was lower than in the more typical temperatures of 2013 in much of the California Current (Leising et al. 2015). This warming was followed by El Niño conditions in late 2015-early 2016 (McClatchie et al. 2016).

The present study investigates the distribution of blue whales and their prey euphausiids around an area of steep bathymetry called Nine Mile Bank (NMB). We address several related questions: (1) Are blue whales associated with NMB? (2) Are the euphausiid species that are preferentially consumed by blue whales more strongly associated with NMB than euphausiid species that are not blue whale prey? (3) Are blue whale prey euphausiid species distributed differently in the water column than nonprey species?

Materials

The study area is a submarine embankment off San Diego, California, called NMB (Fig. 1). NMB is situated nine nautical miles (16.7 km) from Point Loma in San Diego, between the San Diego Trough to the west and the Loma Canyon to the east. The bank feature is parallel to the coastline in a North–South orientation with slopes on both sides approximating 55° from horizontal. We have subdivided our study area into three regions for analysis. The bank itself was defined as shallower than 1150 m to the west and 450 m to the east. The region to the west of the bank will be referred to as offshore, and to the east as inshore. Sampling was conducted on three successive cruises: 26–31 July 2014 aboard the *R/V New*

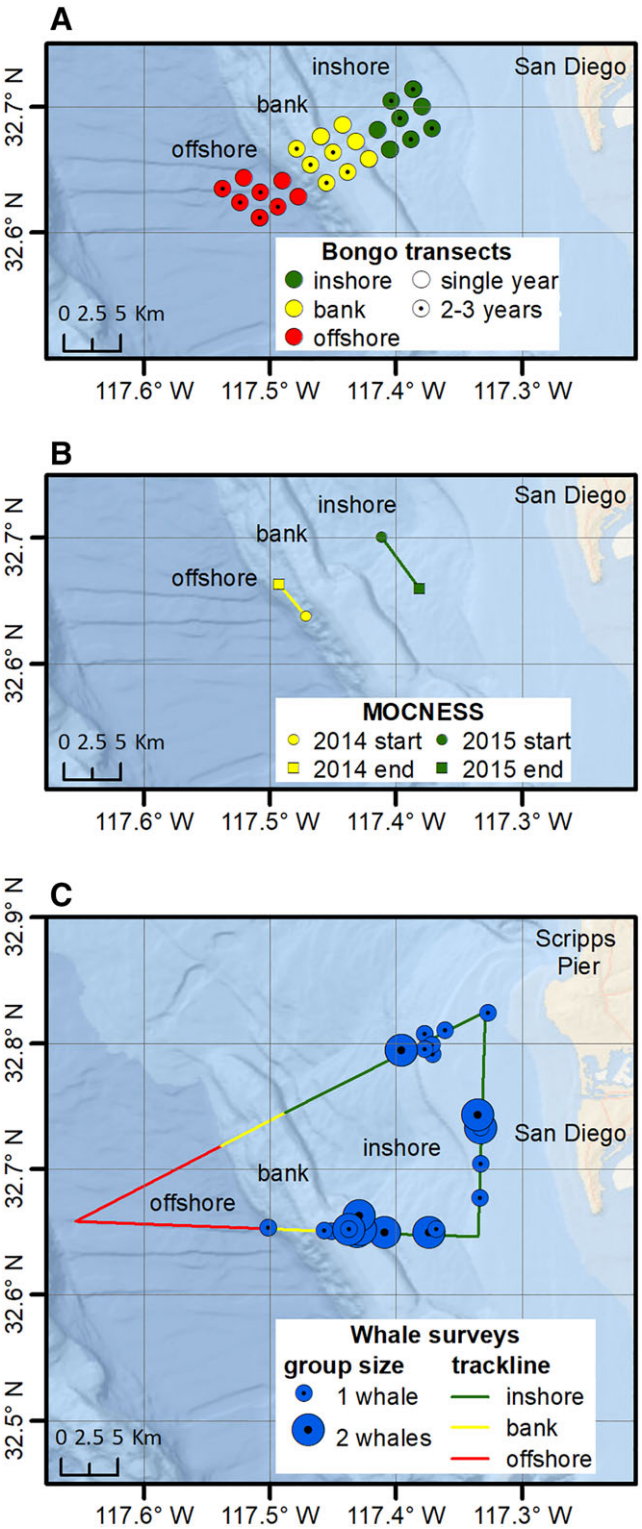

Fig. 1. NMB study area near San Diego, CA. The study area was subdivided into three regions: Inshore, the bank itself, and offshore. **(A)** Bongo tow locations, open circles represent bongo tow locations sampled in 1 yr of the study, circles with a dot inside bongo tow locations sampled in 2 or 3 years. **(B)** MOCNESS tracks and **(C)** whale survey tracklines and sightings. The whale on the westward bank slope in C is within the bank region. Bathymetric map source: Esri, DeLorme, GEBCO, NOAA NGDC, and other contributors.

Horizon, 11–17 June 2015 aboard the *R/V Robert Gordon Sproul*, and 24–25 April 2016 aboard the *R/V Sikuliaq*. The cruises in June and July sampled the available euphausiid prey when blue whales are expected to be present, while April represents contrasting conditions before the whales arrive for the summer season (Burtenshaw et al. 2004; Bissell 2013; Campbell et al. 2015). Sampling in all 3 yr included active multifrequency acoustic methods and bongo net collections. Sampling in 2014 and 2015 also included vertically stratified Multiple Opening/Closing Net and Environmental Sensing System (MOCNESS) tows and collection of whale fecal material (fecal material results are detailed in Nickels et al. 2018). A series of repeated whale visual surveys was conducted in 2015.

Bongo net transects

To assess the distributions of individual euphausiid species with respect to the bank, zooplankton were sampled in a series of bongo net transects on each cruise for summer 2014, 2015, and spring 2016 (Fig. 1A). Transects included tows in the inshore, bank, and offshore regions and proceeded in the offshore (westerly) direction, perpendicular to the long axis of the bank. A 71 cm diameter, 202 μm mesh bongo net was lowered at 50 m min^{-1} to obtain a tow depth of approximately 200 m and retrieved at 20 m min^{-1}, towing obliquely while the ship speed varied between 1 and 2 kts (0.5–1 m s^{-1}) to preserve a 45° wire angle. All tows were conducted between an hour after sunset and an hour before sunrise to minimize net avoidance by larger individuals. A calibrated General Oceanics flow meter was used to record the volume water filtered. Zooplankton were immediately preserved in sodium borate buffered 1.8% formaldehyde after collection.

MOCNESS

To determine the vertical distributions of the individual euphausiid species, we used a MOCNESS (Wiebe et al. 1985) with a 1 m^2 opening and 202 μm mesh in July 2014 and June 2015. Two day and two night tows were performed on both cruises with the start and end locations constant within a cruise. For all tows, the MOCNESS sampled from 350 to 0 m at 10–20 m min^{-1} vertical velocity, ship speed 1 m s^{-1} while towing obliquely. The first five nets in the deeper depth strata each sampled 50 m of the water column, and the shallower four nets each sampled 25 m. In June 2014, we towed along the outer edge downslope of the bank, and in 2015, we moved inshore where *T. spinifera* had been most abundant in 2014 (Fig. 1B).

Many of the euphausiid species of interest are strong daytime net avoiders (Brinton 1967) that could bias our vertical distributions, so we tested whether a strobe light system (Sameoto et al. 1993; Wiebe et al. 2013) would mitigate the effect. The methods and results of this investigation are available as supplemental material. We found strobe lights to have no consistent effect on the euphausiid catches of the MOCNESS for any species investigated, but the strobe lights were activated for all results reported here.

Zooplankton sample analysis

The starboard side of each bongo tow was enumerated for euphausiids. Subsampling was conducted with the use of a Folsom splitter for identification of approximately 200 individuals per tow. Identifications were limited to the top eight most abundant euphausiid species in the Southern California sector of the CCS: *E. pacifica* Hansen, *T. spinifera* Holmes, *Nematoscelis difficilis* Hansen, *Thysanoessa gregaria* Sars, *Euphausia recurva* Hansen, *Euphausia gibboides* Ortmann, *Euphausia eximia* Hansen, and *Nyctiphanes simplex* Hansen (Brinton and Townsend 2003). The first four species are cool-water associated, while the latter four are warm-water associated. Each individual was identified to species and life history phase, and total length was measured from the tip of the rostrum to the tip of the telson (Boden et al. 1955; Brinton 1962; Brinton et al. 2000). Only the results for euphausiids larger than the blue whale lower feeding limit of 10 mm are presented here (Croll et al. 1998; Nickels et al. 2018). Adult and juvenile pelagic *Pleuroncodes planipes* Stimpson were also enumerated to aid in the interpretation of acoustic backscatter. Counts were standardized to individuals 1000 m^{-3}.

Acoustic backscatter

Acoustic backscatter was measured at 38, 120, and 200 kHz with a hull-mounted Simrad EK60 echosounder in 2014 on the *R/V New Horizon*, a pole-mounted Simrad EK60 echosounder in 2015 on the *R/V Robert Gordon Sproul*, and a hull-mounted Simrad EK80 in 2016 on the *R/V Sikuliaq*. The echosounders were calibrated before the start of each cruise using the standard sphere method so that the magnitude of backscattering can be compared between surveys and instruments (Foote et al. 1987). All frequencies were transmitted simultaneously every 2 s with a 1.024 ms pulse length. Acoustic surveys were conducted between 1 h after sunrise and 1 h before sunset so that euphausiid distributions would reflect the daytime feeding period of blue whales (Croll et al. 1998; Fiedler et al. 1998; Calambokidis et al. 2007; Oleson et al. 2007). Each survey crossed the bank between two and eight times at ship speeds of 5–8 kts (~ 2.6–4 m s^{-1}).

Acoustic backscatter was analyzed in Myriax Echoview 4 software. Background noise was removed following De Robertis and Higginbottom (2007), with a signal-to-noise threshold of 5 dB. Data were thresholded at −70 dB to remove weak scattering. This threshold may have excluded some weak scattering from euphausiids in addition to noise; however, the distribution of dense aggregations that would serve as prey for blue whales remained intact. Euphausiid-like backscattering (ELB) was identified utilizing the empirical multifrequency classification Z-score method of De Robertis et al. (2010) based on the difference in volume backscattering strength (ΔS_v) between frequencies, which is sometimes referred to as dB

differencing. Values were allowed to vary 2 standard deviations from the mean expected ΔS_v of De Robertis et al. (2010). Backscatter was classified as euphausiid-like if $\Delta S_{v,\ 120–38}$ was 13.8 ± 5.8 dB, $\Delta S_{v,\ 200–38}$ was 16.3 ± 5.8 dB, and $\Delta S_{v,\ 200–120}$ was 2.3 ± 2.8 dB. While the size distribution of euphausiids is smaller at NMB, values from De Robertis et al. (2010) were the closest match from the literature and are used as a reasonable approximation in the absence of sufficient direct measurements in this study. The Z-score, or normal deviate, was used to estimate confidence in the identification by summarizing the deviations of the observed from expected ΔS_v.

Analysis of concurrent acoustic backscatter and MOCNESS sampling revealed that dB differencing failed to distinguish the backscattering caused by euphausiids from that of pelagic red crabs (*P. planipes*), which first reappeared in this region in small numbers in 2014 and were abundant in 2015 and 2016. Despite its success in separating *P. planipes* from *N. simplex* off Mexico, the difference in scattering intensity at 120 kHz (Gomez-Gutierrez and Robinson 2006) was also ineffective because layers of *P. planipes* confirmed by MOCNESS sampling did not have a stronger acoustic backscattering strength than euphausiid layers. To solve this problem, the Echoview 4 school detection module was used to isolate *P. planipes* in masked echograms passed through a 5 × 5 dilation filter to make the aggregations more contiguous for detection. Schools must have been greater than −70 dB re 1 m^{-1} for at least 40 m along the track and 20 m vertically. These parameters identified *P. planipes* layers but not euphausiid layers as determined from the MOCNESS samples. The school detection was then applied to all acoustic echograms. Differentiation was possible during the day, when the two taxa occupied different vertical layers, but not at night when both migrated vertically to the surface and the layers merged.

Further analyses were performed on the 200 kHz echogram with all noneuphausiid-like data removed. We use ELB as an index of euphausiid density because our limited direct sampling of acoustically detected layers and potential exclusion of weaker euphausiid-associated scattering below our threshold cutoff would make biomass calculations questionable. The area backscattering coefficient (s_a) was integrated over the upper 300 m in 500 m segments along the track.

Whale visual surveys

In conjunction with the 2015 cruise, 10 whale visual surveys were completed from 11 June 2015 to 31 July 2015 (Supporting Information Table S1), using a standard line-transect protocol (Burnham et al. 1980; Barlow and Forney 2007; Buckland et al. 2015). Surveys were conducted from a rigid hulled inflatable boat (observation height effectively sea level) traveling at ~ 5 m s^{-1} while on effort. Each survey repeated the same tracklines (Fig. 1C) and included 3–4 observers, including the boat operator and a dedicated record keeper when personnel allowed. Two primary observers each monitored a 90° field of view from the bow to abeam, together covering the 180° forward of the vessel; sightings were also included when first observed by either the boat operator or record keeper. When a whale was spotted, we went off effort in closing mode to confirm species and group size (Barlow 1997). We did not use photo ID to determine whether individual whales were re-sampled. Survey effort was calculated as distance in km on effort along the trackline. All effort was conducted in sea state conditions of Beaufort 3 (wind speed 4–5 m s^{-1}) or less (average 2.1, wind speed 2.5 m s^{-1}) during daylight.

Analytical methods

To determine the density of whales associated with NMB from visual surveys we estimated the blue whale density of all three regions combined using the software Distance 6.2 (Thomas et al. 2010). Barlow (2015) estimated the detection track probability (g(0)) of blue whales in an average Beaufort state of 2, and we used his value of g(0) = 0.748. The detection function model was selected that minimized the value of the Akaike Information Criterion and maximized the goodness of fit. Some encounters were missing information on the distance and/or angle of the sighting. To correct for this deficiency, the effective strip width was calculated without these sightings, the distances were estimated based on the probability density function, and then density of whales was calculated with the full suite of sightings. The effective strip width was 0.99 km.

To compare the occurrence of whales among the inshore, bank, and offshore regions (Fig. 1C), we calculated a comparative encounter rate as:

$$\frac{\text{number of sightings} \times \text{average group size}}{\text{length of transect}}$$

The average group size is the average of the number of whales spotted during each sighting. The comparative encounter rate represents the number of whales sighted per km of distance traveled along the transect within each region. The distance standardization therefore corrects for the differences in survey effort between regions. Heterogeneity among these encounter rates was then tested with a Kruskal–Wallis nonparametric ANOVA using survey days as replicates within each region.

Both the dB differenced echograms and the euphausiid size and species information from the bongo transects were used to determine the distribution of euphausiids with respect to the bank. We visually assessed the echograms and compared the s_a between regions using the Kruskal–Wallis test with the s_a of each 500 m segment within a region as replicates. Each survey was tested separately. Species-specific distributions were determined from the bongo abundances by comparing the abundance of each species between regions and between years using the Kruskal–Wallis test with tows within each region or year as replicates. To evaluate the patchiness of euphausiid-

like scattering, we used the modified Bez's index of Décima et al. (2010) I_{mod}:

$$I_{\mathrm{mod}} = \left[\frac{\sum_i z_i^2}{s\left(\sum_i z_i\right)^2}\right] N$$

The index uses density data and is robust to differential sampling effort between regions. The volume backscattering coefficient (s_v) was used as an index of density (z). The sampling area (s) was 25 m depth by 500 m distance bins. Vertical patchiness was calculated as I_{mod} for each 500 m wide vertical slice of the echogram, with z_i representing the s_v of each 25 m depth bin (N) within a vertical column. Horizontal patchiness for each 25 m high horizontal slice of the echogram was calculated with z_i representing the s_v of each 500 m horizontal span (N) within a depth bin. A mean and standard deviation of I_{mod} were calculated for each region within a survey, as well as for each year of the study. A lower value of patchiness (lower I_{mod}) indicates a more even dispersal of organisms, while higher patchiness (higher I_{mod}) indicates more unevenness, with greater disparity between samples of high and low density. The indexes were then compared using a Kruskal–Wallis test. To assess the vertical distribution of euphausiid sizes and species, we visually assessed the graphical results from the MOCNESS sampling and concurrent dB differenced echograms.

Statistics were performed in R ver. 3.1.2 (R Core Team, 2014), MATLAB ver. 2016b (Mathworks), and SigmaPlot ver. 10.0 (Systat Software).

Results

Whale distribution

A total of 26 blue whales were encountered over the 10 surveys, with between 1 and 5 sighted per day (mean 2.6, 95% CI 0.89; Fig. 1C; Supporting Information Table S1). We did not achieve the recommended minimum sample size of 60 detections (Burnham et al. 1980; Buckland et al. 2015), and this probably contributed to a coefficient of variation of 0.31 for our density estimate, which is relatively large but acceptable for our comparative purposes. The sample size also limited us to conventional distance sampling, because there were not enough data for multiple covariates to be accurate. Models with half normal-cosine and hazard rate-cosine detection functions were indistinguishable. For the total survey area, the density was 21 whales 1000 km^{-2} (95% CI 12–39). Zero whales were encountered offshore (the whale on the westward bank slope in Fig. 1C is within the bank region). While 1.4 times as many whales were encountered per km surveyed on the bank compared with inshore, the difference was not statistically significant ($p > 0.05$, Kruskal–Wallis); however, both the bank and inshore showed higher whale encounters than offshore ($p < 0.05$), suggesting the bank itself and region immediately inshore are preferred blue whale habitat.

Cross-bank prey distribution

The acoustic echograms illustrate the distribution of ELB in the water during the daytime feeding period of blue whales (Fig. 2). Figure 2 depicts vertically resolved ELB (point clouds) and vertically integrated (0–300 m) area backscattering coefficient (s_a, black bars over echograms) in relation to NMB (black line) from representative across-bank sections of each survey. On both dates in July 2014 (Fig. 2A,B), ELB was diffuse throughout the upper 300 m without well-defined vertical layers of elevated concentration. There is some backscatter in Fig. 2A that appears fish school like that was not excluded by our dB differencing or school detection. On three successive days in June 2015 (Fig. 2C–E), ELB occurred in two distinct layers. Lower intensity backscattering was present from approximately 0 to 150 m, while a higher intensity layer occurred deeper than approximately 200 m. Some of the higher intensity backscattering occurred above the NMB plateau at depths shallower than 200 m. The distribution of ELB in April 2016 (Fig. 2F) resembled the vertical layering pattern of June 2015, but without clear association with the shallow water bank region.

The area backscattering coefficient (s_a) represented by the histograms in Fig. 2 is summarized by region relative to NMB for each survey in Fig. 3. In all surveys, s_a was significantly lower offshore than on the bank or inshore ($p < 0.05$). In both July 2014 surveys, ELB was significantly elevated on the bank compared to offshore ($p < 0.05$), and inshore was not significantly different from either (Fig. 3A,B). On 14 and 16 June 2015, ELB was significantly elevated on the bank and inshore compared to offshore (Fig. 3C,E; $p < 0.05$). On 15 June 2015, ELB was significantly different among all three regions with the highest value on the bank, inshore intermediate, and offshore lowest (Fig. 3D; $p < 0.05$). In April 2016, ELB was significantly enhanced inshore compared to both the bank and offshore (Fig. 3F; $p < 0.05$).

Differences in patchiness among the three regions were not consistent (Supporting Information Fig. S1). For example, vertical patchiness was significantly higher offshore than on the bank ($p < 0.05$) on 28 July 2014 (with inshore not different from either), but 2 days later on 30 July 2014, vertical patchiness was highest inshore and all three significantly different from one another ($p < 0.05$). Comparison of vertical and horizontal patchiness among years, however, showed that vertical patchiness was significantly lower in 2014 than both 2015 and 2016 (Supporting Information Fig. S2A; $p < 0.05$). Horizontal patchiness was significantly different among all 3 years (Supporting Information Fig. S2B, $p < 0.05$), with the lowest patchiness in 2014 and the highest in 2016.

The bongo transects evaluate the spatial distributions of individual euphausiid species in relation to NMB (Fig. 4; Supporting Information Fig. S3). The principal prey euphausiid, *T. spinifera* (Fig. 4A) was most abundant inshore in July 2014 compared to both the bank and offshore ($p < 0.05$). In June 2015, *T. spinifera* was more abundant on the bank compared

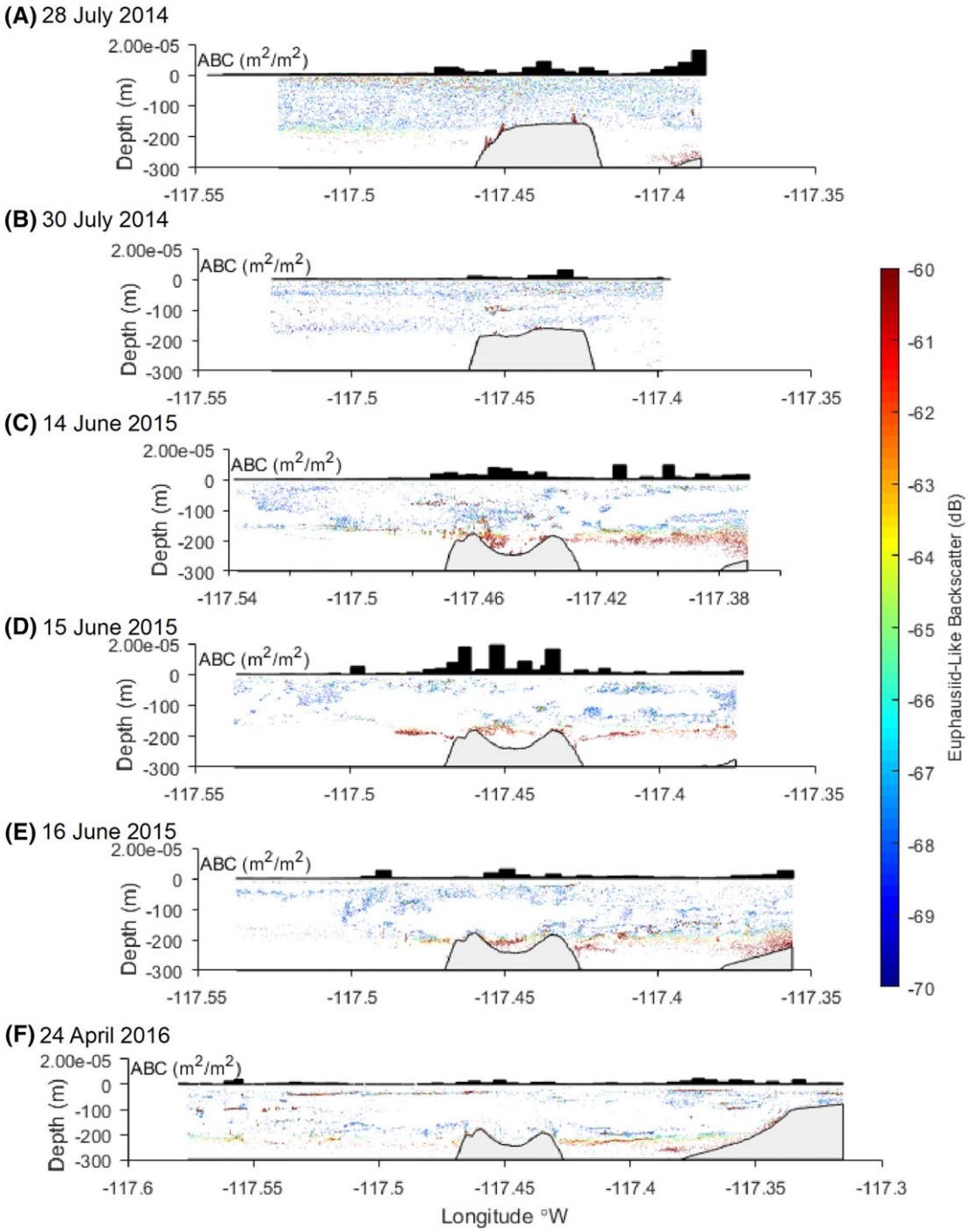

Fig. 2. Representative echograms of ELB (dB) with respect to depth across NMB from **(A,B)** July 2014, **(C–E)** June 2015, and **(F)** April 2016. Bars above the horizontal black lines indicate the area backscattering coefficient (s_a, m^2 m^{-2}) summed from 0–300 m over 500 m distance bins. Gray shading indicates bathymetry.

to offshore ($p < 0.05$), with inshore not significantly different from either. *T. spinifera* was virtually absent in April 2016, when only a few specimens were found on the bank. *E. pacifica* (Fig. 4B) was the most abundant species in July 2014 and June 2015. Like *T. spinifera*, *E. pacifica* was more abundant inshore than on the bank or offshore in July 2014 ($p < 0.05$). There were no significant differences among regions in the abundance of *E. pacifica* in June 2015 or April 2016 (low and variable densities found). For all three regions combined, both *T. spinifera* and *E. pacifica* were more abundant in 2015 than 2014 or 2016 ($p < 0.05$), but the latter 2 yr were not different from one another ($p > 0.05$).

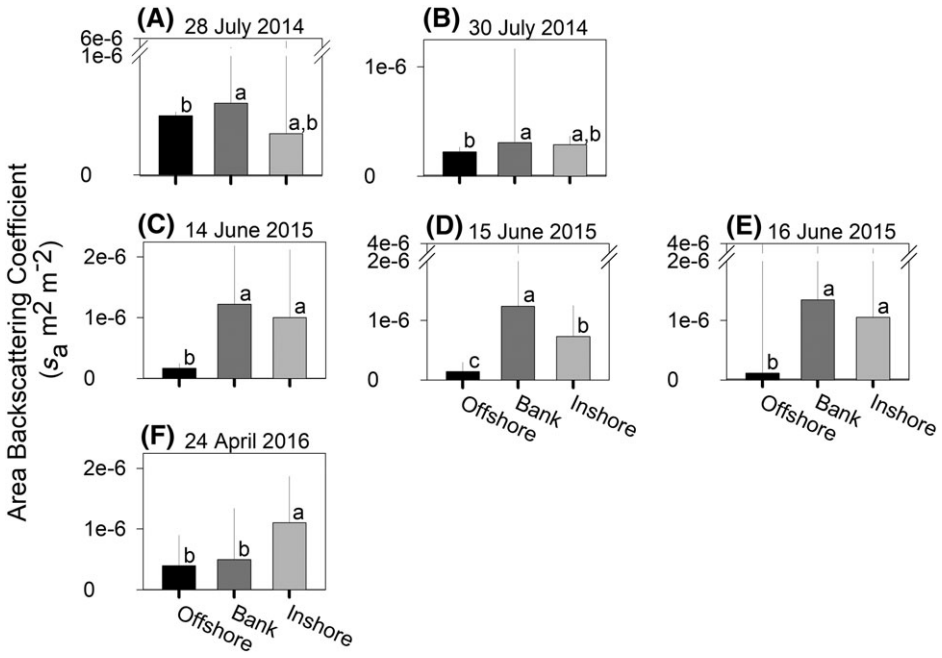

Fig. 3. Mean (± 95%) area backscattering coefficients (s_a, m^2 m^{-2}) for ELB from (A,B) July 2014, (C-E) June 2015, and (F) April 2016. Statistically significant groupings within a survey denoted with a, b, and c ($p < 0.05$).

Euphausiids that make up only a small portion of blue whale diet include cool water-associated species *N. difficilis* and *T. gregaria*, as well as warm water-associated *E. eximia*, *E. gibboides*, *E. recurva*, and *N. simplex* (Supporting Information Fig. S3). *N. difficilis* was more abundant than *T. spinifera* in July 2014 and the most abundant of the eight species in April 2016. In July 2014, *N. difficilis* was significantly more abundant inshore than offshore ($p < 0.05$), with the bank not differing from either. In June 2015, both *N. difficilis* and *T. gregaria* were significantly more abundant offshore and on the bank than inshore ($p < 0.05$). Of the warm water-associated species, only *E. gibboides* showed significant spatial differences in abundance. In July 2014, *E. gibboides* was more abundant offshore than inshore ($p < 0.05$), with the bank not different from either. Only larval *E. recurva* smaller than 10 mm were present during the entire study.

P. planipes, the pelagic red crab, first appeared as a single individual inshore in July 2014, but was much more abundant in June 2015 (Fig. 5A). In 2015, *P. planipes* was significantly more abundant inshore than on the bank or offshore. *P. planipes* was also present in April 2016 (Fig. 5B) but in much lower numbers than in 2015. There was no difference in abundances among inshore, on the bank, or offshore in 2016 ($p > 0.05$).

Vertical prey distribution

The vertical distributions of target prey euphausiids (Fig. 6), nontarget euphausiid prey (Supporting Information Fig. S4) species, and *P. planipes* (Fig. 7) were determined from the MOCNESS tows. *E. pacifica*, a minor blue whale euphausiid prey item, was numerically dominant in both years (Fig. 6B,D, F,H). During the summer 2014 sampling period, *T. spinifera* larvae were present above 150 m both day and night, but no adults large enough to be blue whale prey were collected (Fig. 6A,E). Below 150 m during the day, *E. pacifica* juveniles just smaller than the feeding range of >10 mm were present (Fig. 6B). These *E. pacifica* juveniles migrated to the surface at night (Fig. 6F). A lesser concentration of larger *N. difficilis*, which is not a typical prey species of baleen whales in this region, was collected in 2014 below 250 m (Supporting Information Fig. S4A). In 2015, the largest individuals of the top eight euphausiid species that were present all occupied a layer between 150 and 250 m during the day, with an aggregation of larger size class adult *T. spinifera* between 200 and 250 m (Fig. 6C). The large adult *T. spinifera* reflected in the average were collected during the 14 June 2015 tow, and the layer is apparent in the accompanying echogram as a red band sampled by MOCNESS net 3 (Fig. 8B). Unlike the other species, *T. spinifera* larvae were vertically separated from the adults during the day, with the larvae generally concentrated above 100 m. In contrast, *E. pacifica* and *N. difficilis* larvae were present throughout the upper 300 m in 2015 (Fig. 6D; Supporting Information Fig. S4C). At night, the adult *T. spinifera* and *E. pacifica* vertically migrated toward the surface and spread out in the water column, occupying shallower and more vertically extended depths than during the day (Fig. 6G,H).

P. planipes were not caught in the MOCNESS in 2014, but were present in large numbers in 2015 (Fig. 8). During the day, they occupied the upper 200 m of the water column, and were most abundant between 100 and 150 m (Fig. 7A). At

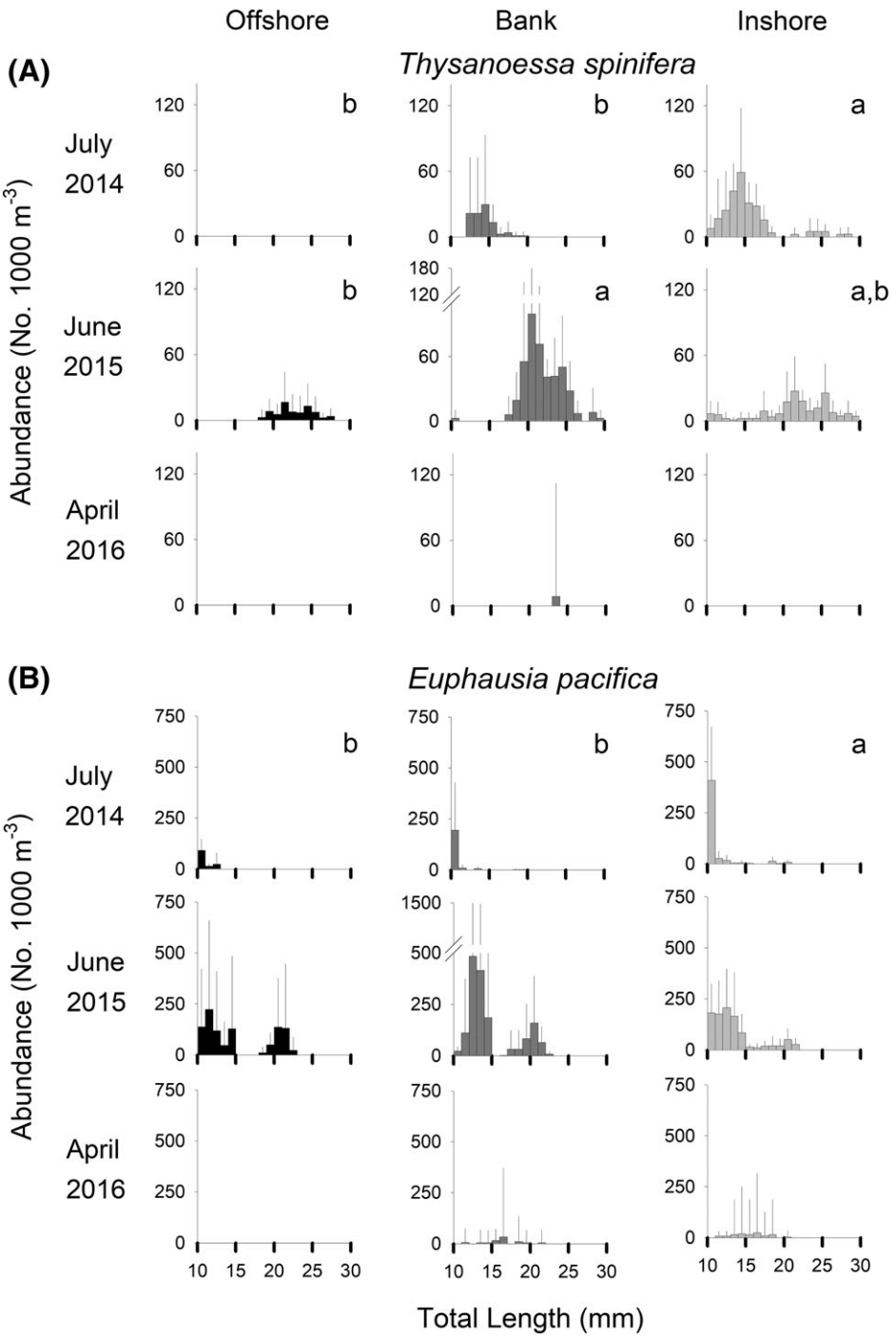

Fig. 4. Mean (± 95%) euphausiid abundance by length class from bongo net transects for target prey species **(A)** *T. spinifera* and **(B)** *E. pacifica*. Statistically significant groupings within a cruise denoted with a and b ($p < 0.05$).

night, they migrated toward the surface like the euphausiids, with their highest numbers in the upper 25 m (Fig. 7B).

Acoustic backscatter was measured concurrently with the MOCNESS tows in both July 2014 and June 2015. In July 2014, ELB was relatively diffuse, without well defined layers (Supporting Information Fig. S5), which is in agreement with the lack of large bodied individuals in the MOCNESS that would have caused strong scattering. In June 2015, the daytime echograms both show two separate layers (Fig. 8A,B). The upper layer spans 25–125 m and the lower layer 175–275 m. Some of the space between the layers in June 2015 was occupied by a layer of *P. planipes* (Fig. 8C,D), which were identified

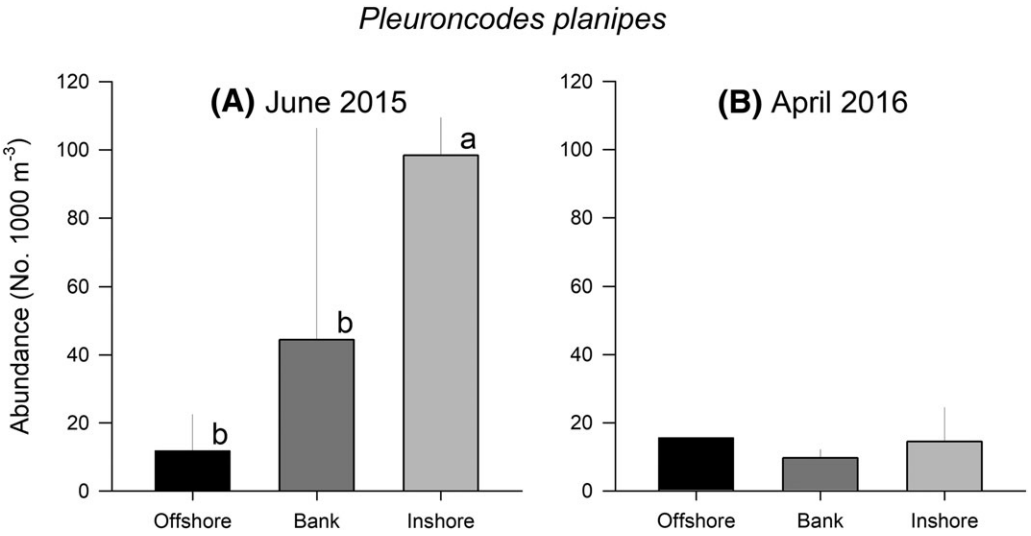

Fig. 5. Mean (± 95%) abundance of *P. planipes* abundance from **(A)** 2015 and **(B)** 2016 bongo net transects. Statistically significant groupings within a cruise denoted with a and b ($p < 0.05$).

in the MOCNESS sampling (Fig. 7A) and removed from the echogram. The most intense ELB was in the deeper layer, where larger adult euphausiids were collected by the MOCNESS (Figs. 6C,D and 8A,B). At night, the most intense backscattering was concentrated near the surface, penetrating to 100 m on 14 June (Fig. 8E) and only 25 m on 15 June (Fig. 8F). The shallow nighttime aggregations were composed of both euphausiids and *P. planipes* (Figs. 7B and 8E,F), and therefore *P. planipes* could not be distinguished from the nighttime ELB.

Discussion

Whale association with NMB

The density of blue whales around NMB was 21 whales 1000 km^{-2} (95% CI 12–39) in 2015. To put this number into perspective, the density of blue whales in larger surveys in the CCS is considerably lower. Barlow and Forney (2007) found a density of 1.36 blue whales 1000 km^{-2} in the area extending 550 km offshore from southern California to Oregon–Washington in the summer and fall. Calambokidis and Barlow (2004) found a blue whale density of 3.49 whales 1000 km^{-2} in their California inshore stratum extending to 230 km offshore. In the southern CCS, as covered by the CalCOFI long-term sampling grid, Campbell et al. (2015) found 3.01 blue whales 1000 km^{-2}. The low end of our CI (12 blue whales 1000 km^{-2}) is still well above this background number, indicating that NMB is an area of increased blue whale density above the surrounding mean. Another well-recognized and well-studied blue whale aggregation center is Monterey Bay, CA, where Croll et al. (2005) found a density of 34 blue whales 1000 km^{-2}. The density of blue whales at NMB, though higher than the ambient average, is lower than the more intense "hotspot" off central California. We note that our density may be an underestimate, as our use of closing mode (in which observers go off effort and break the transect to obtain more certain species identifications) can lead to a negative bias in density estimates even for blue whales (Barlow 1997). We did spot some whales while off effort that were not re-sighted after resuming the trackline, supporting the conclusion that the true density may be even higher.

The high density of blue whales in Monterey Bay could be explained by a high density of prey euphausiids. Croll et al. (2005) found an acoustically inferred concentration of mostly *T. spinifera* and *E. pacifica* in Monterey Bay in summer of 3.9 individuals m^{-3} and 4403 individuals m^{-3} within canyon-associated aggregations. Schoenherr (1991) measured a density of 60.7 individuals m^{-3} within surface swarms and 70.6 individuals m^{-3} within deep layers also around the Monterey Submarine Canyon. The highest densities in the Laurentian Channel baleen whale feeding ground were 4500 individuals m^{-3} of *Thysanoessa raschi* or 1500 individuals m^{-3} of *Meganyctiphanes norvegica* (Cotte and Simard 2005). In the present study at NMB, we found 9.7 individuals m^{-3} above 10 mm size class and 12.1 individuals m^{-3} total of primarily *E. pacifica* and *T. spinifera* within an inshore deep layer sampled by the MOCNESS between 200 and 250 m depth in 2015. The predicted critical threshold for a whale to meet its energetic demands if it feeds continuously is approximately 100 individuals m^{-3} (Goldbogen et al. 2011; Hazen et al. 2015). While our estimate of the density of euphausiids in the deep inshore layer in summer 2015 is considerably below this threshold, our density estimate is from the entire volume of water filtered by a MOCNESS net instead of just over the volume of the euphausiid patch. Acoustically derived density estimates would be higher than net derived estimates because of the difference in water volume within which the euphausiids are presumed to be distributed. The difference in

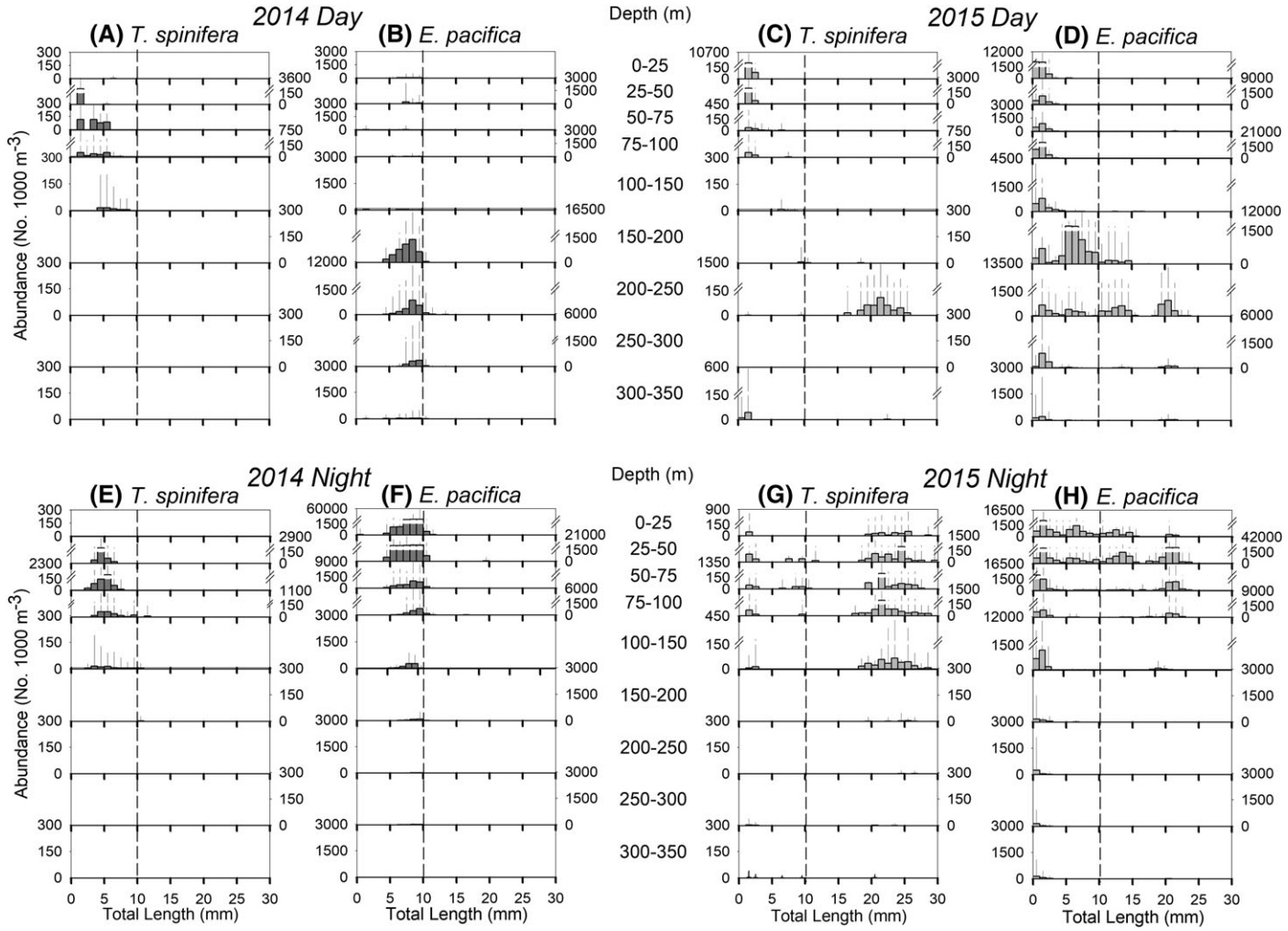

Fig. 6. Vertical distribution of euphausiids by length class from MOCNESS tows for target prey species **(A,C,E,G)** *T. spinifera* and **(B,D,F,H)** *E. pacifica* from (A,B,E,F) July 2014 along the outer edge downslope of the bank and (C,D,G,H) June 2015 inshore. (A–D) daytime tows and (E–H) nighttime tows. Dashed vertical line indicates 10 mm lower size limit of blue whale feeding. Strobe lights were flashing for all nets.

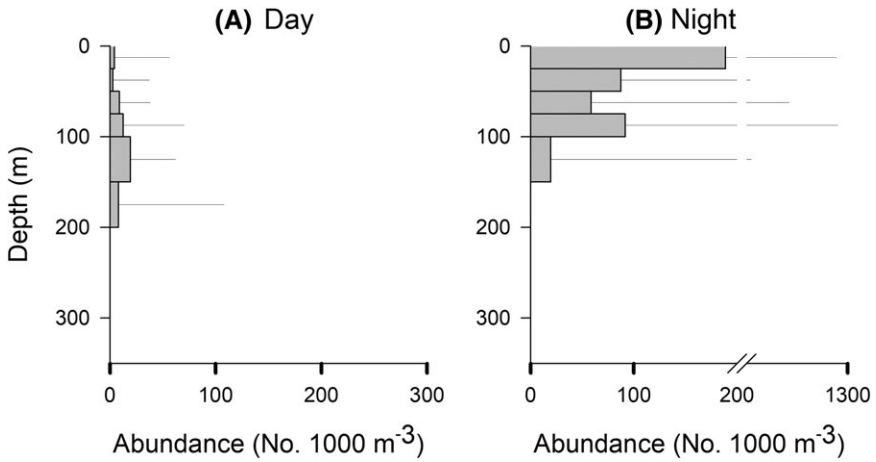

Fig. 7. Mean abundance of *P. planipes* from June 2015 MOCNESS tows inshore of the bank. **(A)** Daytime and **(B)** nighttime tows. Strobe lights were flashing for all nets.

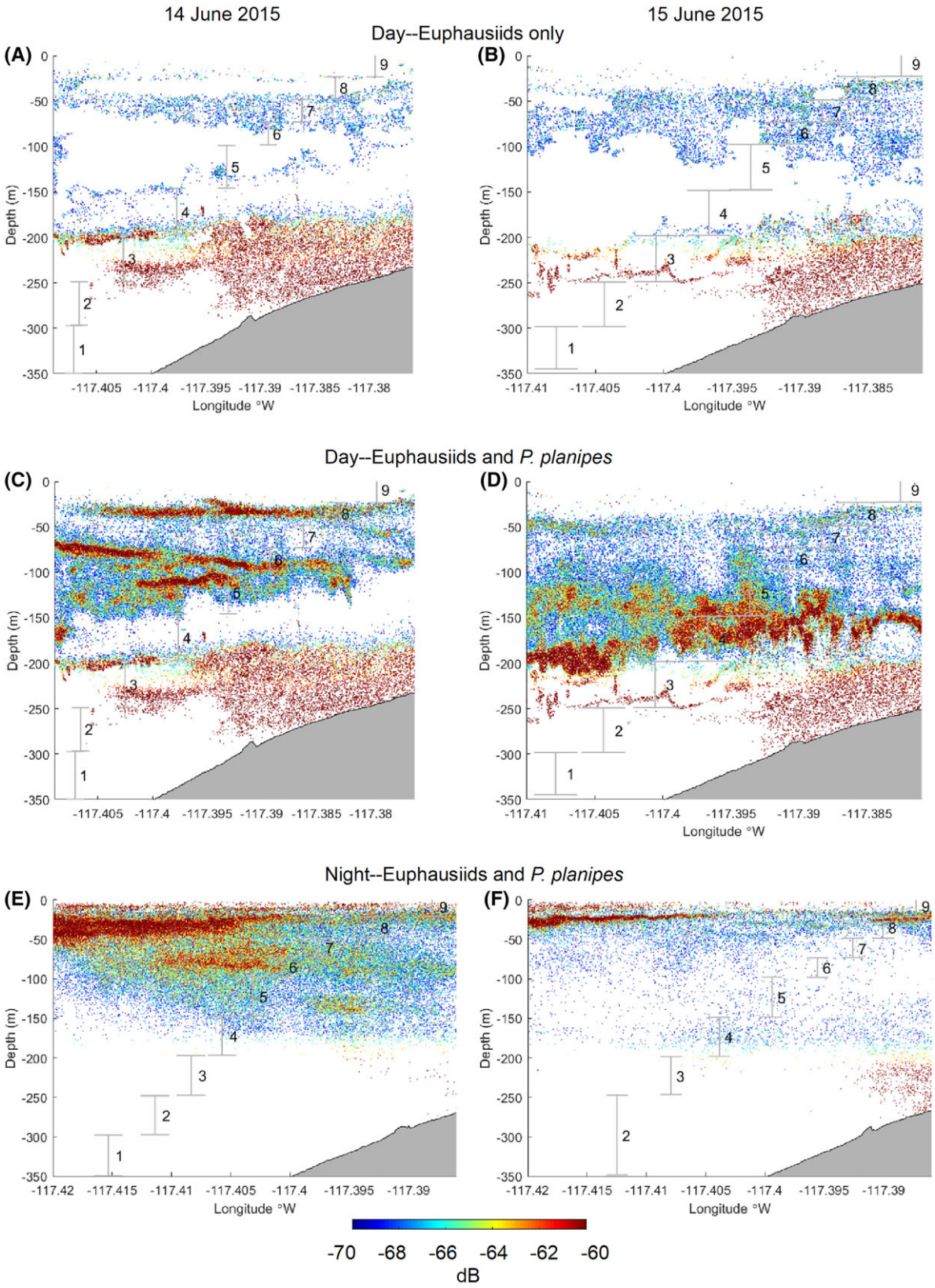

Fig. 8. Echograms of ELB concurrent with MOCNESS sampling from June 2015 inshore of the bank. Gray bars mark the vertical extent of each net through the echogram. **(A,B)** daytime tows with *P. planipes* backscattering removed, **(C,D)** daytime tows with *P. planipes* backscattering included, and **(E,F)** nighttime tows with *P. planipes* backscattering included. Gray shading indicates bathymetry.

volume can be seen in the day echogram from 15 June 2015, where the thin euphausiid layer occupies only a small portion of the depth range sampled by net 3 (Fig. 8B). We did not attempt acoustic density estimates because we were not able to measure target strength in situ. Available target strength models for euphausiids are also designed predominantly for the much larger Antarctic species *Euphausia superba* (e.g., Hewitt and Demer 1993) and may not accurately represent *T. spinifera* and *E. pacifica*. The relative index of ELB was better suited to address our main questions. Whales are more capable than nets of exploiting irregularly shaped euphausiid patches, executing more acrobatic maneuvers in lower density prey patches to maximize prey capture (Goldbogen et al. 2015).

Euphausiid association with NMB

The primary blue whale prey euphausiid, *T. spinifera,* showed highest densities on and inshore of NMB. In contrast, *E. pacifica*, which is much more abundant in the region but forms a minor part of blue whale diets, was not specifically associated with the bank feature. *T. spinifera* is a more nearshore species compared to *E. pacifica*, with a much more restricted geographic range (Brinton 1962). The distribution of the whales more closely matched the distribution of *T. spinifera* than the more abundant *E. pacifica*. The bank feature appears to function as an outer limit for both the whales and high densities of *T. spinifera*, rather than a consistent site of aggregation. This covariation is in agreement with dietary analysis from fecal samples that *T. spinifera* is the strongly preferred prey in the CCS, followed by the more abundant, though generally smaller *E. pacifica* (Schoenherr 1991; Kieckhefer 1992; Croll et al. 1998; Fiedler et al. 1998; Croll et al. 2005; Nickels et al. 2018). Other euphausiid species appear incidentally in the diet when consumed with these two but are not targeted (Nickels et al. 2018).

In 2015, when we censused both blue whales and *T. spinifera,* their spatial distributions covaried. We acknowledge that the whale distribution is likely also responding to other factors. It is unlikely, however, that the whales are aggregating inshore to avoid ship traffic. We encountered many more vessels on and inshore of the bank than offshore. NMB is also a popular fishing and whale watching location, in addition to lying within a naval operation area. While we did not encounter any blue whales offshore of the bank, one was reported from whale watching data (Bissell 2013).

Euphausiid vertical distribution

Our concurrent sampling with the MOCNESS and acoustic echosounders allows us to describe the species-specific distributions of euphausiids available as potential whale prey. In 2015, the diffuse upper layer of daytime ELB corresponded to small euphausiid larvae. The large adults, particularly of *T. spinifera*, were confined to a thin layer of ELB approximately 200 m deep, which corresponds to the average dive depth for blue whales in the area (Goldbogen et al. 2012). This aggregation trails off the edge of another slope that is located inshore of NMB. In closer association with the seafloor is a large area of ELB that the MOCNESS was unable to sample. We do not know what species this aggregation is composed of, but speculate that the seafloor may block whales from executing effective lunges through it, providing refuge for the concentrated euphausiids. The layer of adult euphausiids sampled from slightly deeper water may be composed of individuals advected out of this larger aggregation and made available for whale consumption.

In addition to species preferences, blue whales appear to have a lower size threshold of prey at 10 mm (Croll et al. 1998; Nickels et al. 2018). There are several possible mechanisms for this, including escapement of smaller individuals through the baleen or the inability of hard parts of smaller prey to survive digestion and be detectable in fecal material. Here, we find both support and challenge for a third hypothesis: that the euphausiids are size segregated in the water column. We found evidence for size segregation in primary prey species *T. spinifera* but not in *E. pacifica* or *N. difficilis*. In the vertically stratified samples, the adults of the primary prey *T. spinifera* were vertically separated from their larval phases. A whale targeting a monospecific *T. spinifera* patch would easily encounter and capture only mature adults. However, smaller *E. pacifica* and *N. difficilis* were present throughout the water column, making them also likely to be occasionally ingested along with *T. spinifera*, unless there are micro-scale layers of *T. spinifera* on a vertical scale smaller than the intervals of our MOCNESS sampling. This possibility, or the existence of species-specific aggregation behaviors that render *T. spinifera* more susceptible to detection, bears attention in the future.

Euphausiid patchiness

Patchiness and density can often be more informative than areal backscattering in describing the parameters of the prey field most relevant to a foraging predator (Benoit-Bird et al. 2013). The same number of individual euphausiids spread evenly throughout a volume of water would require a whale to expend more energy to consume than that number of individuals tightly aggregated into patches in only some part of the volume. Both *T. spinifera* and *E. pacifica* adults can form dense aggregations (Brinton 1981; Endo 1984; Smith and Adams 1988), allowing whales to capture more individuals in a single lunge than if the prey were more dispersed (Schoenherr 1991; Fiedler et al. 1998). We expected that ELB would be more patchily distributed where the whales were present than where they were not. On the scale explored here, we did not find a consistent difference of patchiness among regions. We did, however, find lower vertical patchiness in 2014 compared to the other years studied and an increasing horizontal patchiness with year. Due to the timing of sampling, 2014 was assessed in more extreme climactic conditions than 2015. A Northeast Pacific-wide warm anomaly occurred in 2014 and was pronounced before the summer sampling period (Zaba and Rudnick 2016). That anomaly had

relaxed somewhat by June 2015, and the El Niño of late 2015–2016 had not yet fully developed (Jacox et al. 2016). In spring 2016, when El Niño was still expressed but waning, ELB was also patchy, but the spring abundance was much lower and therefore would not have provided adequate food resources. These interannual differences could also be the result of monthly or weekly variation in patchiness, at shorter timescales than our yearly sampling scheme resolved and so these results should be viewed with some caution.

The blue whale preferred prey *T. spinifera* has been documented to form dense surface aggregations of mature adults (Brinton 1981; Smith and Adams 1988). Surface swarms of *M. norvegica* in the North Atlantic may also form around bathymetric crests and attract euphausiid predators including humpback and fin whales (Stevick et al. 2008). Such aggregations are thought to be particularly efficient food resources for lunge feeding whales (Schoenherr 1991; Fiedler et al. 1998). We were not able to sample a surface aggregation either with quantitative nets or active acoustics during this study, but one was observed inshore of the bank during the whale visual survey on 23 June 2015. Sampling with a dip net revealed that it was composed of adult *T. spinifera*. Such surface aggregations may be of particular interest for a feeding whale, but prey density is a more important factor in feeding efficiency than prey depth (Goldbogen et al. 2011). The deeper layers more routinely observed would still be attractive prey if they are composed of the correct prey species and sizes in sufficient density. Blue and humpback whales do track euphausiid ascent in the evening, but cease feeding when euphausiids are close to the surface at night (Fiedler et al. 1998; Calambokidis et al. 2007; Goldbogen 2011; Burrows et al. 2016).

P. planipes intrusion

In addition to the euphausiids, *P. planipes* subadults were found in MOCNESS tows during 2015. MOCNESS tows revealed high abundances of *P. planipes* concentrated at shallower depths than adult *T. spinifera* during the day. Acoustic echograms also showed these layers. We found an elevated population of *P. planipes* inshore of the bank in 2015. Pelagic red crabs were found to aggregate similarly to euphausiids inshore of NMB and could have served as an alternate food source for visiting baleen whales. In southern California waters high numbers of pelagic red crabs stranded along the coast and were observed within the water column and in the gut contents of many pelagic predators during 2014–2016 (McClatchie et al. 2016). The presence of this food item in many cases will serve as a less calorically valuable supplement to the diets of many seabirds, fish, and whales during warm periods when sardine, and anchovy abundances are depressed (Alverson 1963). In blue whale fecal samples collected inshore of the bank in 2015, we detected some minor incidental feeding upon red crab through remains of an intact claw and a few antennae. Humpback whales are known to feed upon another munid crab *Munida gregaria* in the Antarctic (Matthews 1937).

Implication for interannual variation

We observed an influx of El Niño indicators including *P. planipes* and *N. simplex* during 2015, which were also reported during the 1997–1998 El Niño in Monterey Bay (Marinovic et al. 2002). Based on historic evidence from the CalCOFI, we would expect lower abundances of *T. spinifera* and *E. pacifica* during an El Niño (Brinton and Townsend 2003, Lilly and Ohman 2018). During non-El Niño years, when abundances of euphausiid species that constitute more preferred blue whale prey are higher, we would expect NMB to be an even more suitable stopover location for baleen whale feeding. Additionally, the persistence of available whale prey, despite these anomalous conditions, could mean that NMB and areas like it serve as food refuges along the blue whale migration route, such as Monterey Bay during the 1997–1998 El Niño (Benson et al. 2002; Marinovic et al. 2002). The reliability of these areas would be important to foraging whales. The warm water anomalies could also mean that the present study represents a conservative estimate of the food resources available and baleen whale presence during normal conditions.

Conclusions

Both blue whales and their primary prey species *T. spinifera* were more abundant on or inshore of NMB than offshore. The bank serves as an offshore limit of increased prey abundance that may draw the whales to the area. The minor prey species *E. pacifica*, while much more abundant and dispersed more evenly around the bank, had less influence on the distribution of whales. Euphausiids large enough to be whale prey were concentrated in a thin layer between 200 and 250 m during the day, corresponding to previously documented daytime feeding depths of blue whales, and *T. spinifera* adults and larvae were vertically separated. The tighter link between the distributions of the whales and their preferred, but less abundant, prey *T. spinifera* highlights the importance of species-specific analysis of euphausiid distributions. The persistence of NMB as a site of elevated blue whale abundance through anomalously warm conditions in the CCS may make it a food refuge for whales during periods of lower productivity.

References

Alverson, F. G. 1963. The food of yellowfin and skipjack tunas in the eastern tropical Pacific Ocean. Inter-American Tropical Tuna Commission Bull. **7**: 293–396.

Bailey, H., B. R. Mate, D. M. Palacios, L. Irvine, S. J. Bograd, and D. P. Costa. 2009. Behavioural estimation of blue whale movements on the Northeast Pacific from state-space model analysis of satellite tracks. Endanger. Species Res. **10**: 93–106. doi:10.3354/esr00239

Barlow, J. 1997. Preliminary estimates of cetacean abundance off California, Oregon, and Washington based on a 1996 ship survey and comparisons of passing and closing modes. SWFSC Administrative Report LJ-97-11.25. U.S. Department of Commerce.

Barlow, J. 2015. Inferring trackline detection probabilities, g(0), for cetaceans from apparent densities in different survey conditions. Mar. Mamm. Sci. **31**: 923–943. doi:10.1111/mms.12205

Barlow, J., and K. Forney. 2007. Abundance and population density of cetaceans in the California current ecosystem. Fish. Bull. **105**: 509–526.

Benoit-Bird, K. and others 2013. Prey patch patterns predict habitat use by top marine predators with diverse foraging strategies. PLoS One **e53348**: 8. doi:10.1371/journal.pone.0053348

Benson, S. R., D. A. Croll, B. B. Marinovic, F. P. F. P. Chavez, and J. T. Harey. 2002. Changes in the cetacean assemblage of a coastal upwelling ecosystem during El Niño 1997-98 and La Niña 1999. Prog. Oceanogr. **54**: 279–291. doi:10.1016/S0079-6611(02)00054-X

Bissell, M. W. 2013. Using volunteered geographic information to model blue whale foraging habitat, Southern California bight. University of Southern California. doi:10.1038/503333a

Boden, B. P., M. W. Johnson, and E. Brinton. 1955. The Euphausiacea (Crustacea) of the North Pacific. Bull. Scripps Inst. Oceanogr. **6**: 287–400.

Brinton, E. 1962. The distribution of Pacific euphausiids. Bull. Scripps Inst. Oceanogr. **8**: 51–269.

Brinton, E. 1967. Vertical migration and avoidance capability of euphausiids in the California current. Limnol. Oceanogr. **12**: 451–483. doi:10.4319/lo.1967.12.3.0451

Brinton, E. 1981. Euphausiid distributions in the California current during the warm winter-spring of 1977-78, in context of a 1949-1966 time series. CalCOFI Rep. **22**: 135–154.

Brinton, E., M. D. Ohman, A. W. Townsend, M. D. Knight, and A. L. Bridgeman. 2000. Euphausiids of the world ocean. Marine species identification portal. DOI: 10.1023/A:1008941110816

Brinton, E., and A. Townsend. 2003. Decadal variability in abundances of the dominant euphausiid species in southern sectors of the California current. Deep-Sea Res. Part II **50**: 2449–2472. doi:10.1016/S0967-0645(03)00126-7

Buckland, S., E. Rexstad, T. Marques, and C. Oedekoven. 2015. Distance sampling: methods and applications. Springer. doi:10.2106/JBJS.O.00276

Burnham, K. P., D. R. Anderson, and J. L. Laake. 1980. Estimation of density from line transect sampling of biological populations. Wildl. Monogr. **72**: 7–202. doi:10.1002/bimj.4710240306

Burrows, J. A., D. W. Johnston, J. M. Straley, E. M. Chenoweth, C. Ware, C. Curtice, S. L. DeRuiter, and A. S. Friedlaender. 2016. Prey density and depth affect the fine-scale foraging behavior of humpback whales *Megaptera novaeangliae* in Sitka sound, Alaska, USA. Mar. Ecol. Prog. Ser. **561**: 245–260. doi:10.3354/meps11906

Burtenshaw, J., E. M. Oleson, J. A. Hildebrand, M. A. McDonald, R. K. Andrew, B. M. Howe, and J. A. Mercer. 2004. Acoustic and satellite remote sensing of blue whale seasonality and habitat in the Northeast Pacific. Deep-Sea Res. Part II. **51**: 967–986. doi:10.1016/j.dsr2.2004.06.020

Calambokidis, J., and J. Barlow. 2004. Abundance of blue and humpbac whales in the eastern North Pacific estimated by capture-recapture and line-transect methods. Mar. Mamm. Sci. **20**: 63–85. doi:10.1111/j.1748-7692.2004.tb01141.x

Calambokidis, J. and others 2007. Insights into the underwater diving, feeding, and calling behavior of blue whales from a suction-cup-attached video-imaging tag (CRITTERCAM). Mar. Technol. Soc. J. **41**: 19–29. doi:10.4031/002533207787441980

Campbell, G. S., L. Thomas, K. Whitaker, A. B. Douglas, J. Calambokidis, and J. A. Hildebrand. 2015. Inter-annual and seasonal trends in cetacean distribution, density and abundance off southern California. Deep-Sea Res. Part II **112**: 143–157. doi:10.1016/j.dsr2.2014.10.008

Cotte, C., and Y. Simard. 2005. Formation of dense krill patches under tidal forcing at whale feeding hot spots in the St. Lawrence estuary. Mar. Ecol. Prog. Ser. **288**: 199–210. doi:10.3354/meps288199

Croll, D., and others. 1998. An integrated approach to the foraging ecology of marine birds and mammals. Deep-Sea Res. Part II **45**: 1353–1371. doi:10.1016/S0967-0645(98)00031-9

Croll, D., B. Marinovic, S. Benson, F. P. Chavez, N. Black, R. Ternullo, and B. Tershy. 2005. From wind to whales: Trophic links in a coastal upwelling system. Mar. Ecol. Prog. Ser. **289**: 117–130. doi:10.3354/meps289117

De Robertis, A., and I. Higginbottom. 2007. A post-processing technique to estimate the signal-to-noise ratio and remove echosounder background noise. ICES J. Mar. Sci. **64**: 1282–1291. doi:10.1093/icesjms/fsm112

De Robertis, A., D. R. McKelvey, and P. H. Ressler. 2010. Development and application of an empirical multifrequency method for backscatter classification. Can. J. Fish. Aquat. Sci. **67**: 1459–1474. doi:10.1139/F10-075

Décima, M., M. D. Ohman, and A. DeRobertis. 2010. Body size dependence of euphausiid spatial patchiness. Limnol. Oceanogr. **55**: 777–788. doi:10.4319/lo.2009.55.2.0777

Dorman, J. G., W. J. Sydeman, M. Garcia-Reyes, R. A. Zeno, and J. A. Santora. 2015. Modeling krill aggregations in the central-northern California current. Mar. Ecol. Prog. Ser. **528**: 87–99. doi:10.3354/meps11253

Endo, Y. 1984. Daytime surface swarming of *Euphausia pacifica* (Crustacea: Euphausiacea) in the Sanriku coastal waters off northeastern Japan. Mar. Biol. **79**: 269–276. doi:10.1007/BF00393258

Fiedler, P. and others 1998. Blue whale habitat and prey in the California Channel Islands. Deep-Sea Res. Part II. **45**: 1781–1801. doi:10.1016/S0967-0645(98)80017-9

Foote, K. G., H. P. Knudsen, G. Vestnes, D. N. MacLennan, and E. J. Simmonds. 1987. Calibration of acoustic instruments for fish density estimation: A practical guide. ICES Cooperative Res. Rep. **144**: 1–69.

Genin, A. 2004. Bio-physical coupling in the formation of zooplankton and fish aggregations over abrupt topographies. J. Mar. Syst. **50**: 3–20. doi:10.1016/j.jmarsys.2003.10.008

Goldbogen, J. A., J. Calambokidis, E. Oleson, J. Potvin, N. D. Pyenson, G. Schorr, and R. E. Shadwick. 2011. Mechanics, hydrodynamics and energetics of blue whale lunge feeding: Efficiency dependence on krill density. J. Exp. Biol. **214**: 131–146. doi:10.1242/jeb.048157

Goldbogen, J. A., and others. 2012. Scaling of lunge-feeding performance in rorqual whales: Mass-specific energy expenditure increases with body size and progressively limits diving capacity. Funct. Ecol. **26**: 216–226. doi:10.1111/j.1365-2435.2011.01905.x

Goldbogen, J. A., E. L. Hazen, A. S. Friedlaender, J. Calambokidis, S. L. DeRuiter, A. K. Stimpert, and B. L. Southall. 2015. Prey density and distribution drive the three-dimensional foraging strategies of the largest filter feeder. Funct. Ecol. **29**: 951–961. doi:10.1111/1365-2435.12395

Goldbogen, J. A., D. Cade, J. Calambokidis, A. S. Friedlaender, J. Potvin, P. S. Segre, and A. J. Werth. 2017. How baleen whales feed: The biomechanics of engulfment and filtration. Annu. Rev. Mar. Sci. **9**: 367–386. doi:10.1146/annurev-marine-122414-033905

Gomez-Gutierrez, J., and C. Robinson. 2006. Tidal current transport of epibenthic swarms of the euphausiid *Nyctiphanes simplex* in a shallow, subtropical bay on Baja California peninsula, Mexico. Mar. Ecol. Prog. Ser. **320**: 215–231. doi:10.3354/meps320215

Hazen, E. L., A. S. Friedlaender, and J. A. Goldbogen. 2015. Blue whales (*Balaenoptera musculus*) optimize foraging efficiency by balancing oxygen use and energy gain as a function of prey density. Sci. Adv. **1**: e1500469. doi:10.1126/sciadv.1500469

Hewitt, R., and D. Demer. 1993. Dispersion and abundance of Antarctic krill in the vicinity of Elephant Island in the 1992 austral summer. Mar. Ecol. Prog. Ser. **99**: 29–39. doi:10.3354/meps099029

Jacox, M. G., E. L. Hazen, K. D. Zaba, D. L. Rudnick, C. A. Edwards, A. M. Moore, and S. J. Bograd. 2016. Impacts of the 2015-2016 El Nino on the California current system: Early assessment and comparison to past events. Geophys. Res. Lett. **43**: 7072–7080. doi:10.1002/2016GL069716

Kawamura, A. 1980. A review of food of balaenopterid whales. Sci. Rep. Whales Res. Inst. **32**: 155–197.

Kieckhefer, T. R. 1992. Feeding ecology of humpback whales in continental shelf waters near Cordell Bank. San Jose State Univ.

Leising, A. and others 2015. State of the California current 2014-15: Impacts of the warm-water "blob". CalCOFI Rep. **56**: 31–68.

Lesage, V., K. Gavrilchuk, R. Andrews, and R. Sears. 2017. Foraging areas, migratory movements and winter destinations of blue whales from the western North Atlantic. Endanger. Species Res. **34**: 27–43. doi:10.3354/esr00838

Lilly, L. E., and M. D. Ohman. 2018. CCE IV: El Niño-related zooplankton variability in the southern California Current System. Deep-Sea Res. Part I. doi:10.1016/j.dsr.2018.07.015

Marinovic, B., D. Croll, N. Gong, S. Benson, and F. Chavez. 2002. Effects of the 1997-1999 El Nino and La Nina events on zooplankton abundance and euphausiid community composition within the Monterey Bay coastal upwelling system. Prog. Oceanogr. **54**: 265–277. doi:10.1016/S0079-6611(02)00053-8

Matthews, L. H. 1937. The humpback whale, *Megaptera nodosa*. Discovery Rep. **17**: 7–92.

McClatchie, S. and others 2016. State of the California current 2015–16: Comparisons with the 1997–98 El Niño. CalCOFI Rep. **57**: 5–61.

McDonald, M. A., S. L. Mesnick, and J. A. Hildebrand. 2006. Biogeographic characterization of blue whale song worldwide: Using song to identify populations. J. Cetacean Res. Manag. **8**: 55–65.

Nickels, C. F., L. M. Sala, and M. D. Ohman. 2018. The morphology of euphausiid mandibles used to assess predation by blue whales in the southern sector of the California current system. J. Crustac. Biol. doi:10.1093/jcbiol/ruy062

Oleson, E., J. Calambokidis, W. Burgess, M. McDonald, C. LeDuc, and J. Hildebrand. 2007. Behavioral context of call production by eastern North Pacific blue whales. Mar. Ecol. Prog. Ser. **330**: 269–284. doi:10.3354/meps330269

Sameoto, D., N. Cochrane, and A. Herman. 1993. Convergence of acoustic, optical, and net-catch estimates of euphausiid abundance: Use of artificial light to reduce net avoidance. Can. J. Fish. Aquat. Sci. **50**: 334–346. doi:10.1139/f93-039

Santora, J. A., W. J. Sydeman, I. D. Schroeder, B. K. Wells, and J. C. Field. 2011. Mesoscale structure and oceanographic determinants of krill hotspots in the California current: Implications for trophic transfer and conservation. Prog. Oceanogr. **91**: 397–409. doi:10.1016/j.pocean.2011.04.002

Schoenherr, J. R. 1991. Blue whales feeding on high concentrations of euphausiids around Monterey submarine canyon. Can. J. Zool. **69**: 583–594. doi:10.1139/z91-088

Smith, S. E., and P. B. Adams. 1988. Daytime surface swarms of *Thysanoessa spinifera* (Euphausiacea) in the Gulf of the Farrallones, California. Bull. Mar. Sci. **42**: 76–84.

Stevick, P., L. Incze, S. Kraus, S. Rosen, N. Wolff, and A. Baukus. 2008. Trophic relationships and oceanography on and around a small offshore bank. Mar. Ecol. Prog. Ser. **363**: 15–28. doi:10.3354/meps07475

Thomas, L. and others 2010. Distance software: Design and analysis of distance sampling surveys for estimating population size. J. Appl. Ecol. **47**: 5–14. doi:10.1111/j.1365-2664.2009.01737.x

Wiebe, P. H., G. L. Lawson, A. C. Lavery, N. J. Copley, E. Horgan, and A. Bradley. 2013. Improved agreement of net and acoustical methods for surveying euphausiids by mitigating avoidance using a net-based LED strobe light system. ICES J. Mar. Sci. **70**: 650–664. doi:10.1093/icesjms/fst005

Wiebe, P. H., A. W. Morton, A. M. Bradley, R. H. Backus, J. E. Craddock, V. Barber, T. J. Cowles, and G. R. Flierl. 1985. New development in the MOCNESS, an apparatus for sampling zooplankton and micronecton. Mar. Biol. **87**: 313–323. doi:10.1007/BF00397811

Zaba, K., and D. Rudnick. 2016. The 2014-2015 warming anomaly in the Southern California current system observed by underwater gliders. Geophys. Res. Lett. **43**: 1241–1248. doi:10.1002/2015GL067550

Acknowledgments

The authors would like to thank the many people who made this study possible, including the science parties of SKrillEx I, II, and III, CCE-LTER P1408, and the crews of the R/V *New Horizon*, R/V *Robert Gordon Sproul*, R/V *Sikuliaq*, and R/V *Melville.* The whale visual surveys were made possible by boat operators Brett Pickering and Josh Jones as well as the volunteer observers, with guidance and assistance from John Hildebrand and Jay Barlow. Visual surveys were conducted under NMFS Permit 17312 issued to the Scripps Institution of Oceanography. Pete Davison, Alex DeRobertis, Jian Liu, and Tony Koslow provided help and guidance with the acoustical calculations. Tais Castellano, Han Zou, Shelbi Richardson, Doris Stumps, and Jui-Yuan Chang provided additional laboratory assistance. Annie Townsend taught us euphausiid species identification. Dave Jensen provided valuable visualization and statistical code. Mike Landry and Jon Shurin provided additional comments throughout the process. The anonymous referees provided constructive suggestions. This work was supported by the U.S. National Science Foundation via the California Current Ecosystem LTER site (OCE-10-26607 and OCE-16-37632), UC Ship Funds, and the Scripps Institution of Oceanography Graduate Department.

Conflict of Interest

None declared.

Submitted 8 March 2018
Revised 12 July 2018
Accepted 31 August 2018

Associate editor: Kelly Benoit-Bird

Table S1: Blue whale sightings

	Group Size		
Date	Offshore	Bank	Inshore
11-Jun-15	0	1	2
		2	
16-Jun-15	0	0	2
18-Jun-15	0	0	2
			2
23-Jun-15	0	0	1
			2
25-Jun-15	0	0	2
2-Jul-15	0	0	1
			1
			1
14-Jul-15	0	0	1
15-Jul-15	0	0	1
16-Jul-15	0	1	0
21-Jul-15	0	2	0
		1	
		1	

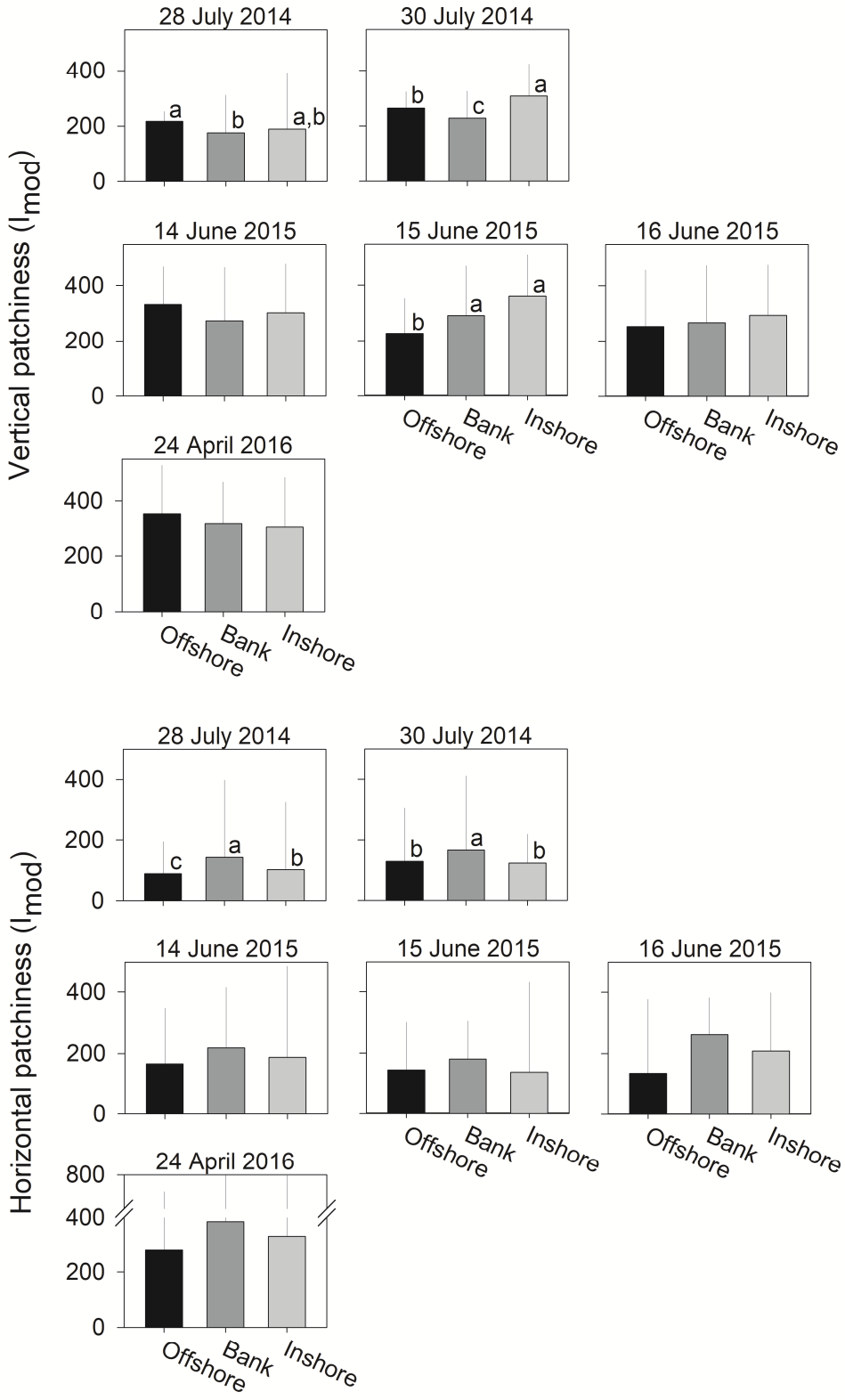
Vertical patchiness (I_{mod})
28 July 2014
30 July 2014
14 June 2015
15 June 2015
16 June 2015
24 April 2016
400
200
0
a
b
a,b
b
c
a
b
a
a
Offshore
Bank
Inshore
Horizontal patchiness (I_{mod})
800
c
a
b
b
a
b

Figure S1: Mean (±95%) patchiness (I_{mod}) in the vertical and the horizontal dimension from acoustic surveys. Statistically significant groupings within a survey denoted with a, b, c ($p<0.05$).

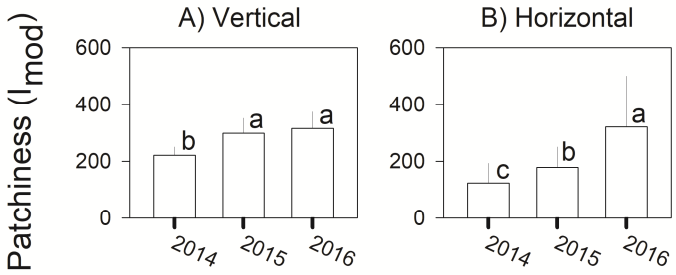

Figure S2: Mean (±95%) patchiness (I_{mod}) in (A) the vertical and (B) the horizontal dimension from acoustic surveys. Statistically significant groupings within a survey denoted with a, b, c ($p<0.05$).

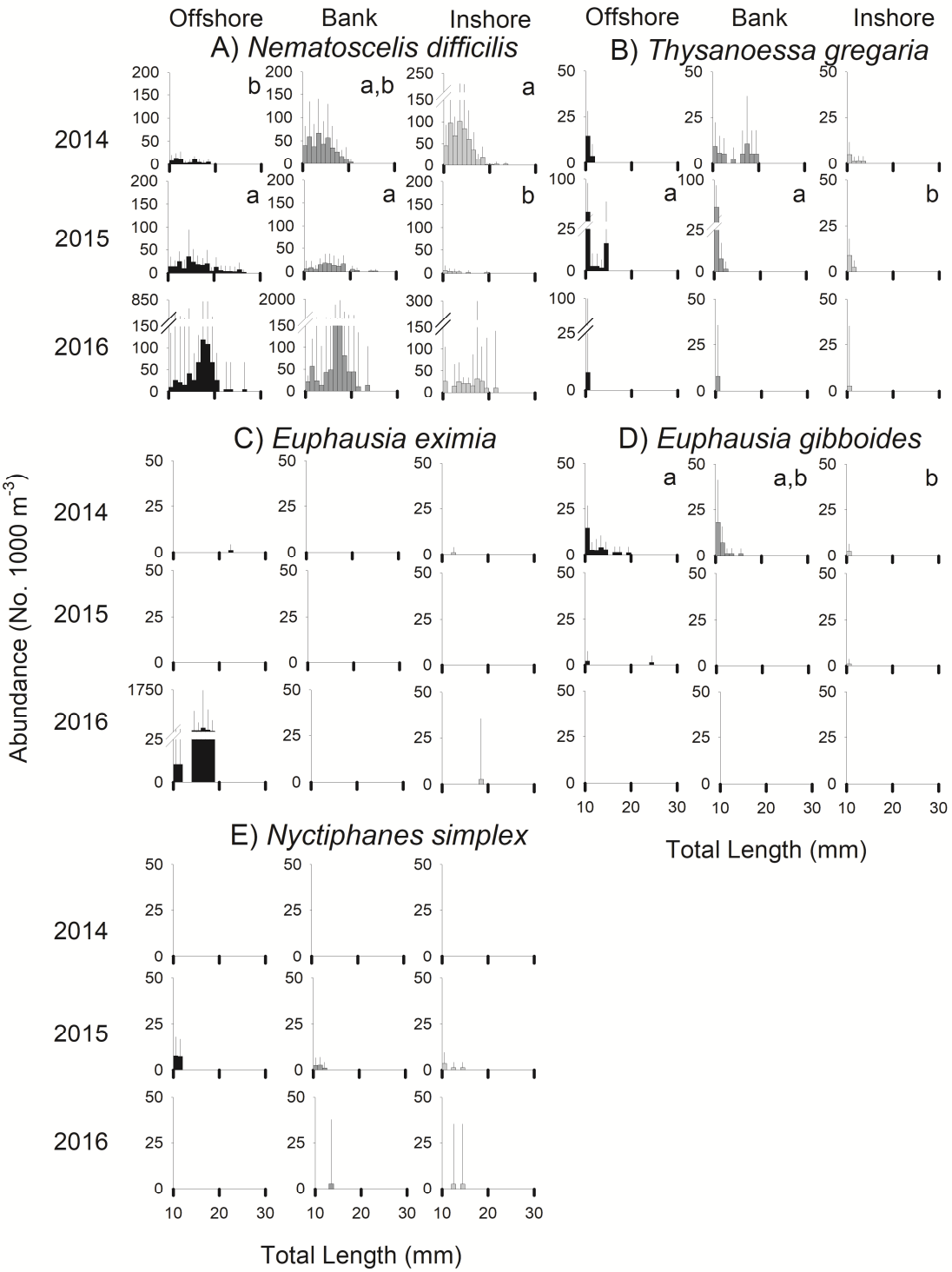

Figure S3: Mean (±95%) euphausiid abundance by length class from bongo net transects for incidental prey species (A) *Nematoscelis difficilis,* (B) *Thysanoessa gregaria,* (C) *Euphausia eximia,* (D) *Euphausia gibboides,* and (E) *Nyctiphanes simplex*. Statistically significant groupings within a cruise denoted with a, b ($p<0.05$).

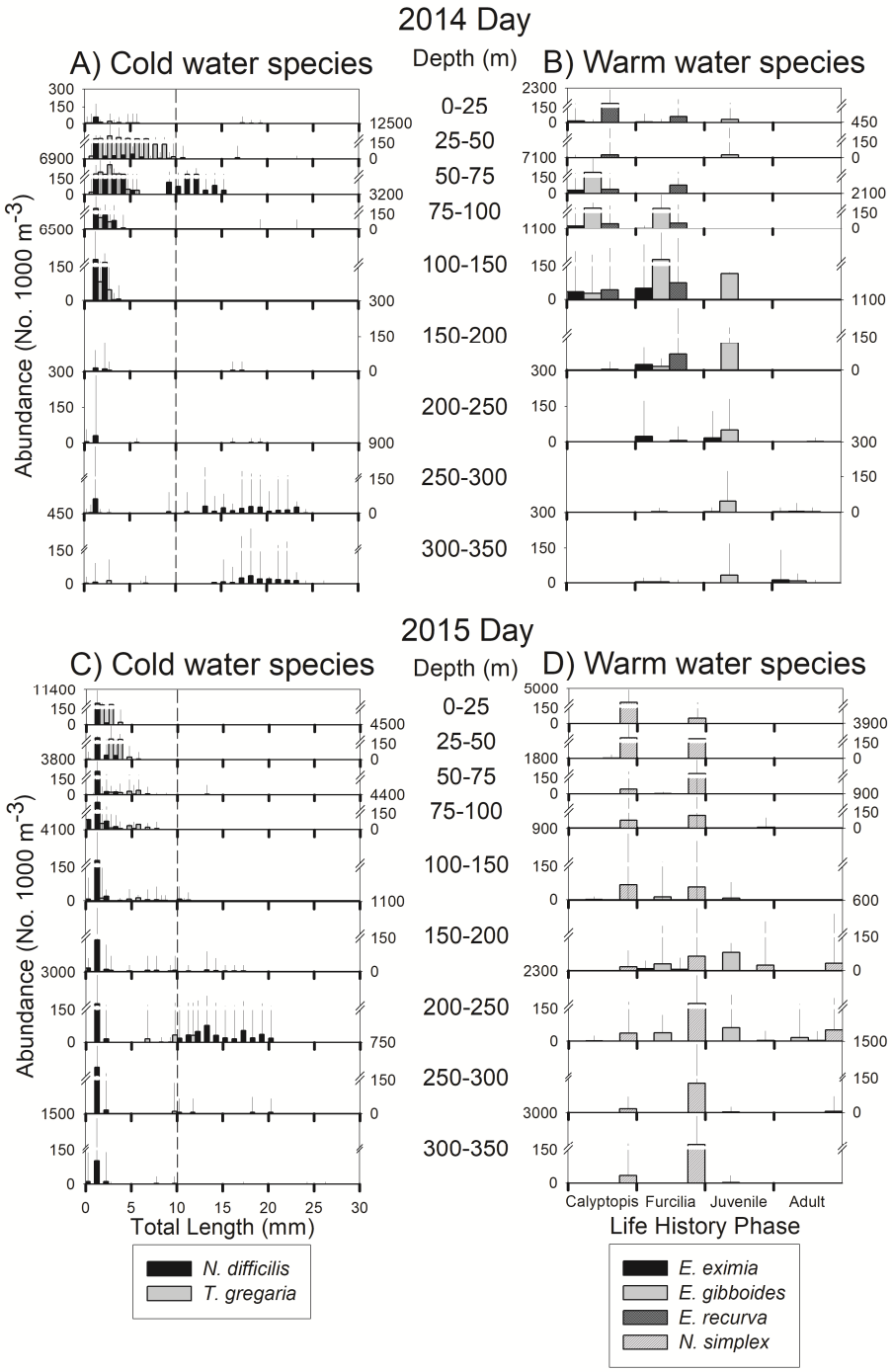

Figure S4: Vertical distribution of euphausiids by length class from MOCNESS tows for incidental or non-prey species associated with the (A,C) cold water assemblage (*N. difficilis*, *T. gregaria*) and (B,D) warm water assemblage (*E. eximia*, *E. gibboides*, *E. recurva*, *N. simplex*) from daytime tows. (A,B) from July 2014 along the outer edge downslope of the bank and (C,D) June 2015 along inshore of the bank. Dashed vertical line indicates 10 mm lower size limit of blue whale feeding. Strobe lights were flashing for all nets.

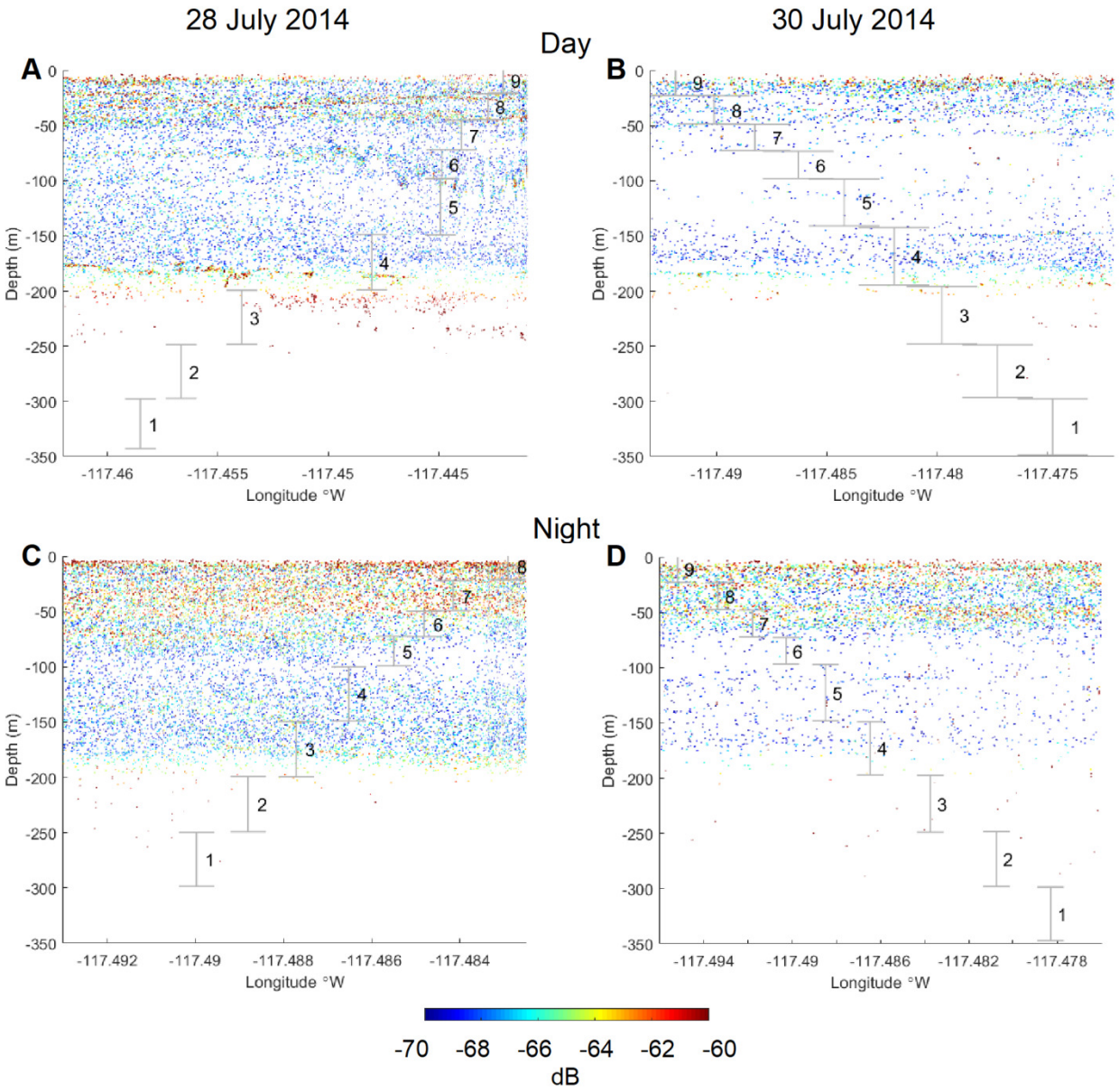

Figure S5: Echograms of euphausiid-like backscattering concurrent with MOCNESS sampling from July 2014 along the offshore slope of the bank. Gray bars mark the vertical extent of each net through the echogram. (A, B) Daytime and (C,D) nighttime tows.

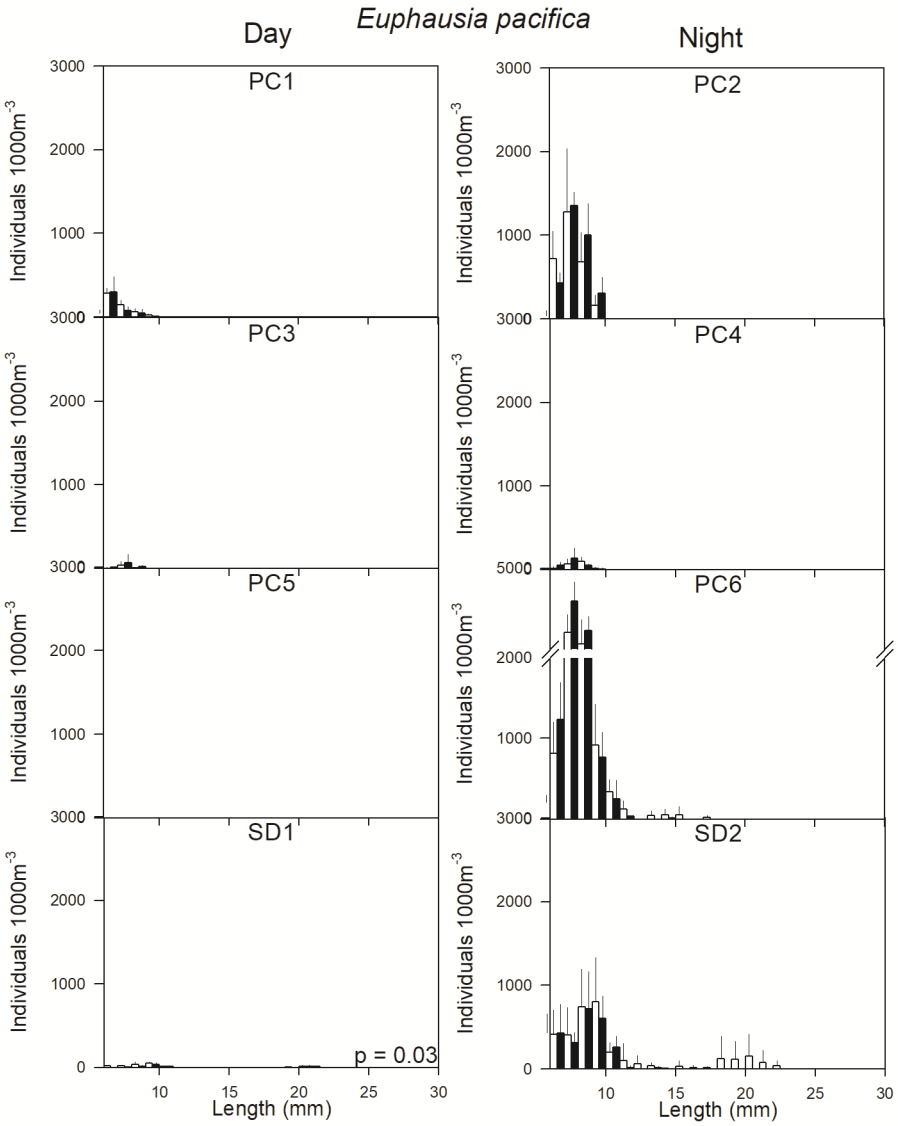

Figure S6: Mean (±95%) *Euphausia pacifica* abundance by length class collected by MOCNESS near Point Conception (PC) and San Diego (SD) with strobe lights on (open bars) and off (filled bars). P value listed for significant Kruskal Wallis test.

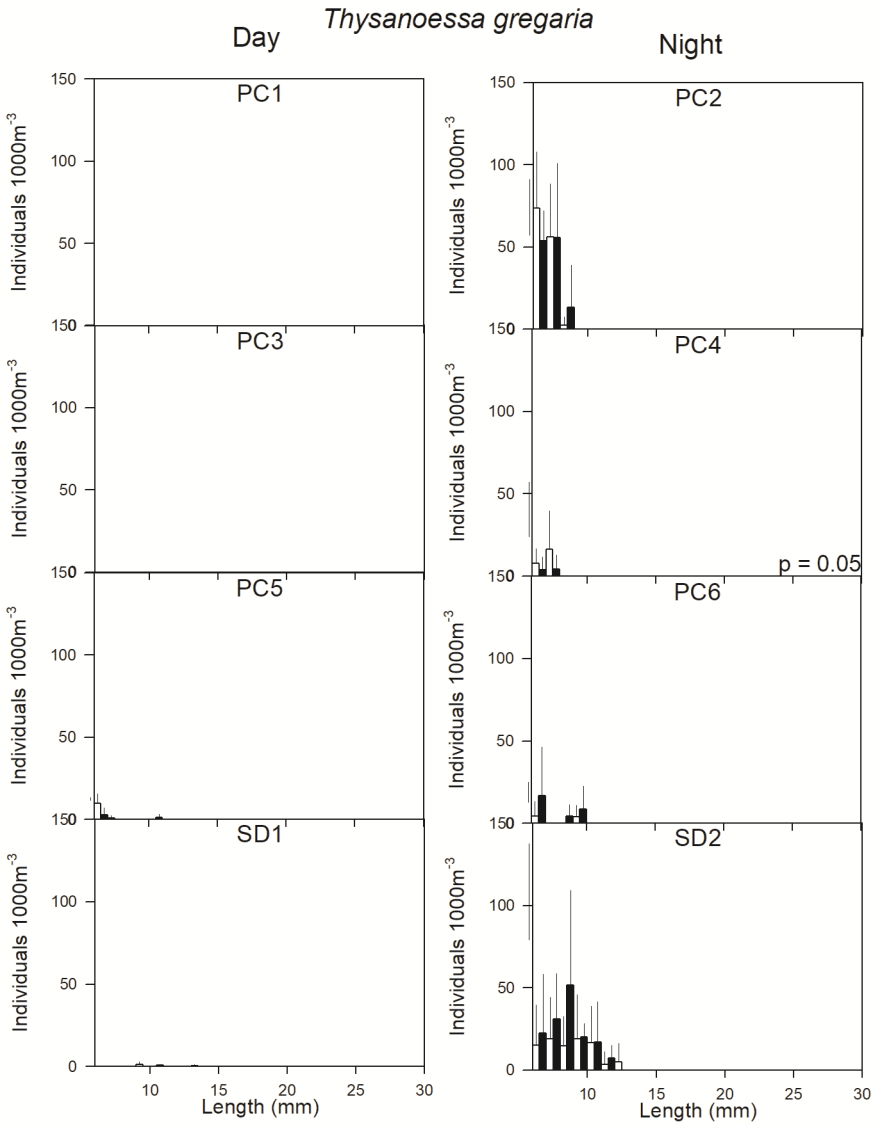

Figure S7: Mean (±95%) *Thysanoessa gregaria* abundance by length class collected by MOCNESS near Point Conception (PC) and San Diego (SD) with strobe lights on (open bars) and off (filled bars). P value listed for significant Kruskal Wallis test.

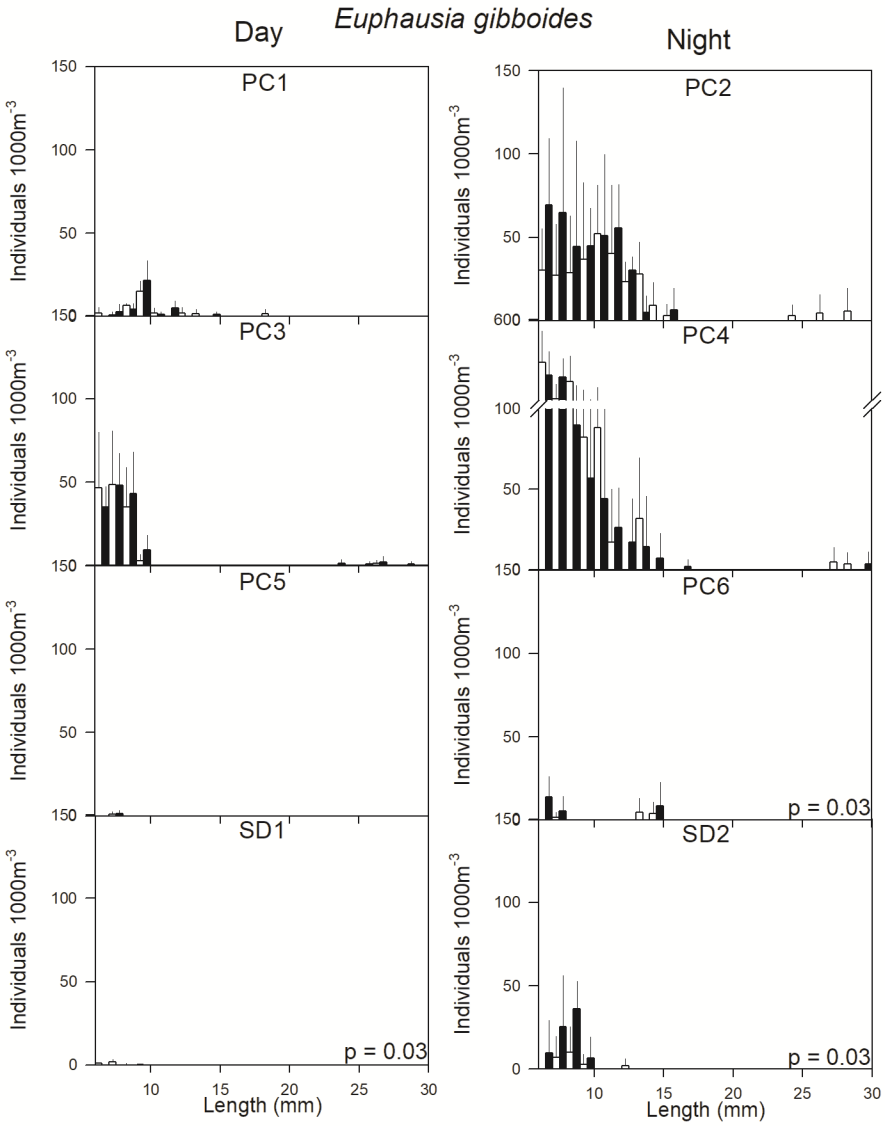

Figure S8: Mean (±95%) *Euphausia gibboides* abundance by length class collected by MOCNESS near Point Conception (PC) and San Diego (SD) with strobe lights on (open bars) and off (filled bars). P value listed for significant Kruskal Wallis test.

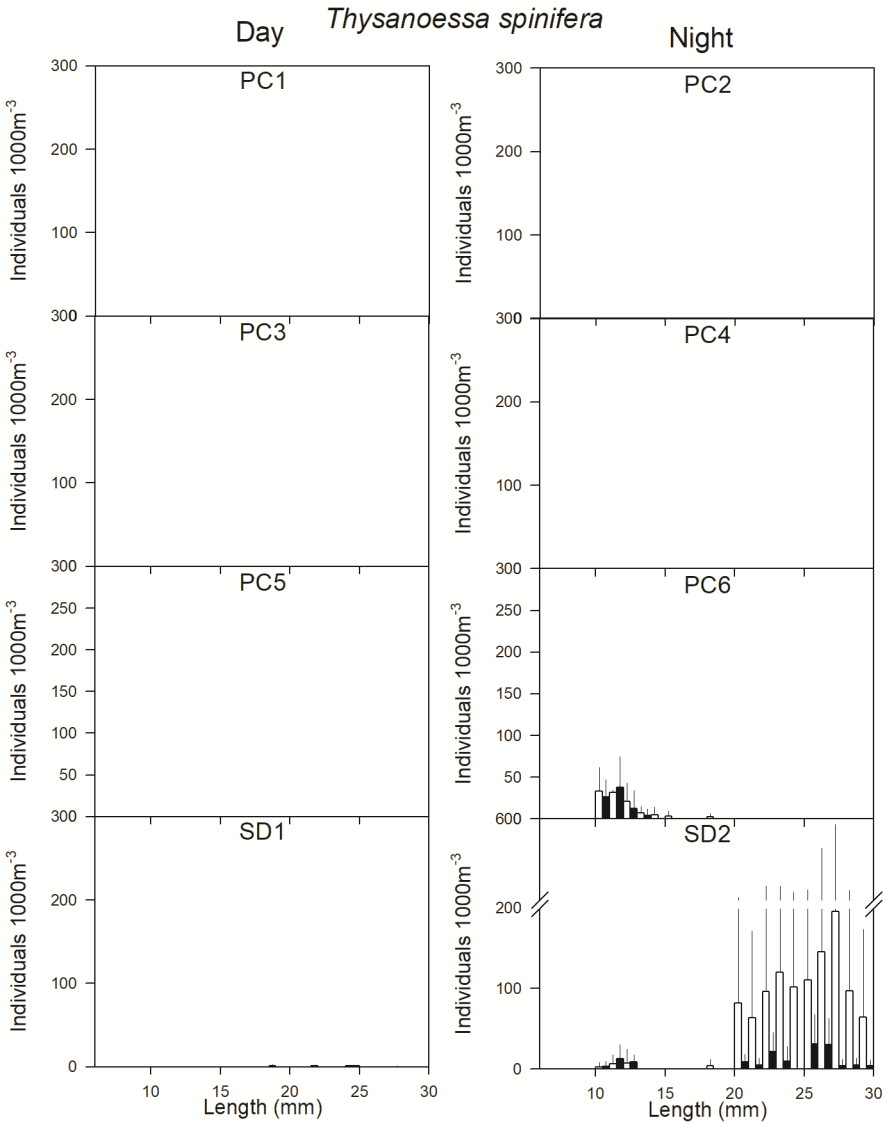

Figure S9: Mean (±95%) *Thysanoessa spinifera* abundance by length class collected by MOCNESS near Point Conception (PC) and San Diego (SD) with strobe lights on (open bars) and off (filled bars).

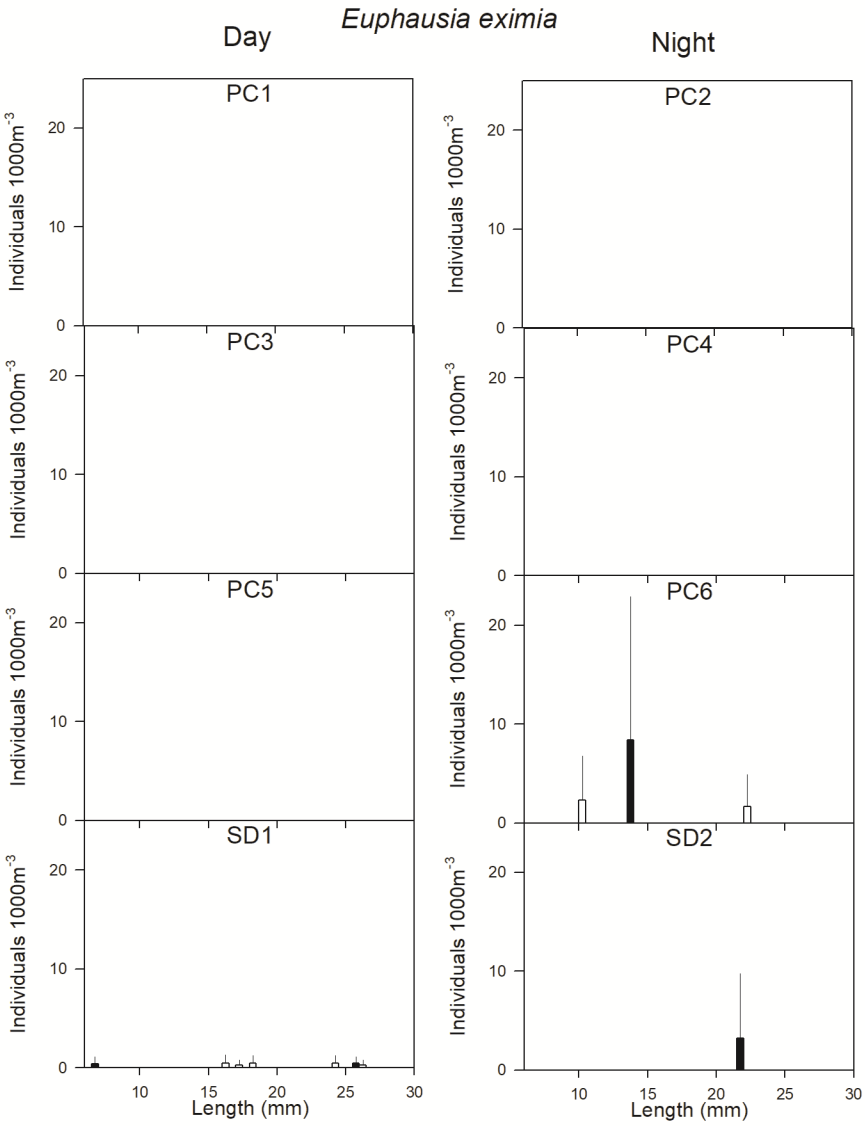

Figure S10: Mean (±95%) *Euphausia eximia* abundance by length class collected by MOCNESS near Point Conception (PC) and San Diego (SD) with strobe lights on (open bars) and off (filled bars).

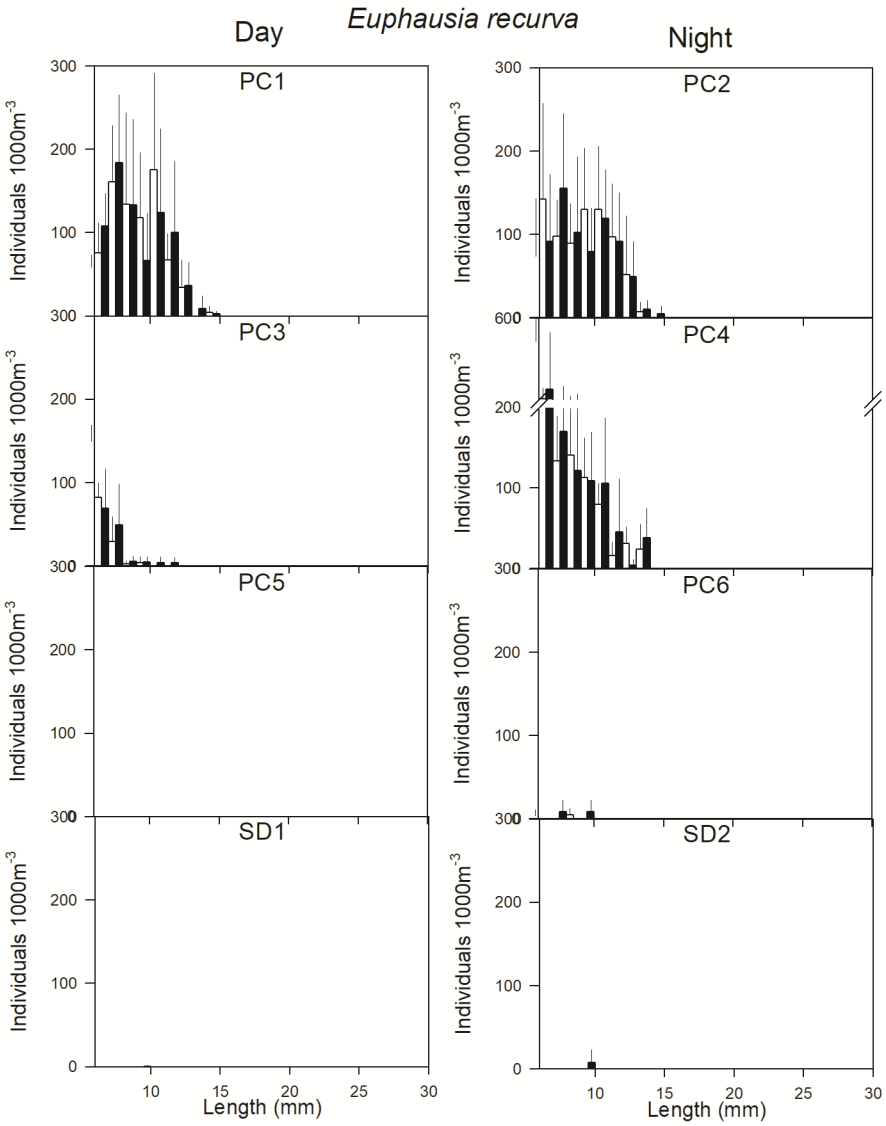

Figure S11: Mean (±95%) *Euphausia recurva* abundance by length class collected by MOCNESS near Point Conception (PC) and San Diego (SD) with strobe lights on (open bars) and off (filled bars).

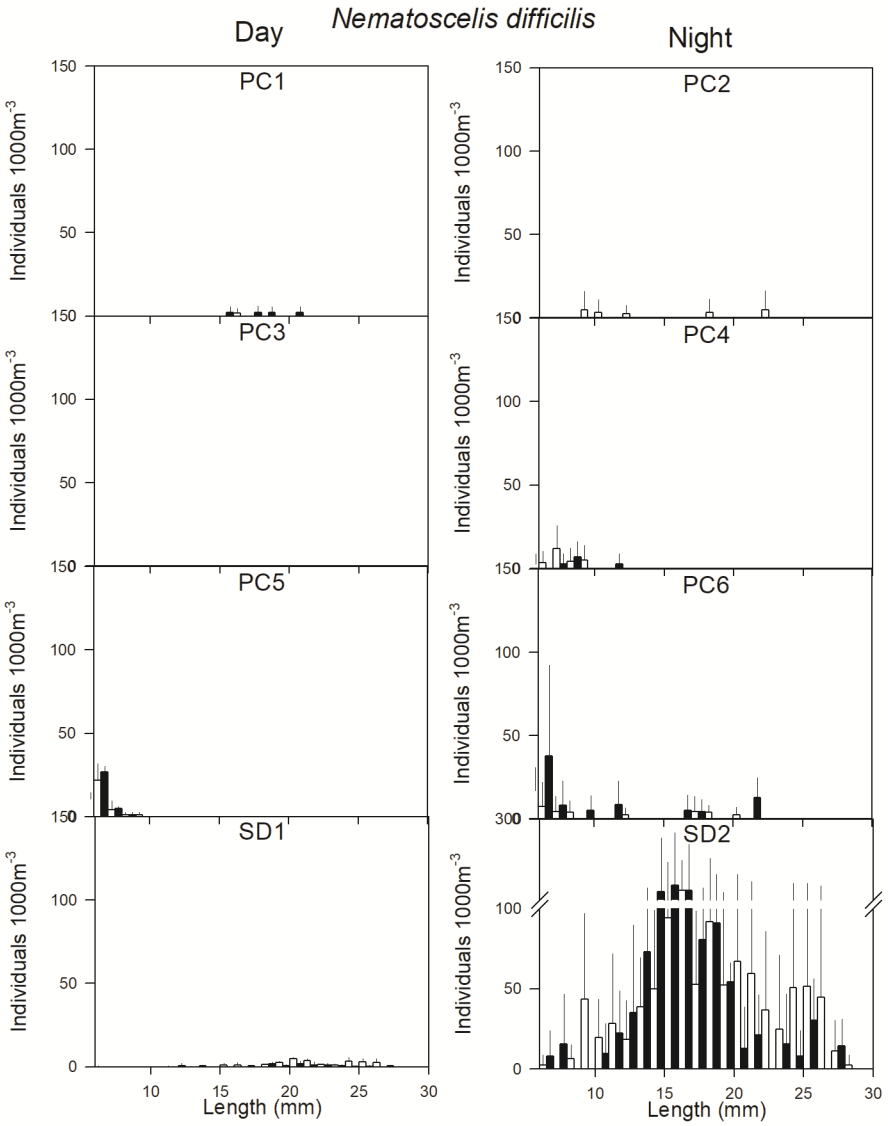

Figure S12: Mean (±95%) *Nematoscelis difficilis* abundance by length class collected by MOCNESS near Point Conception (PC) and San Diego (SD) with strobe lights on (open bars) and off (filled bars).

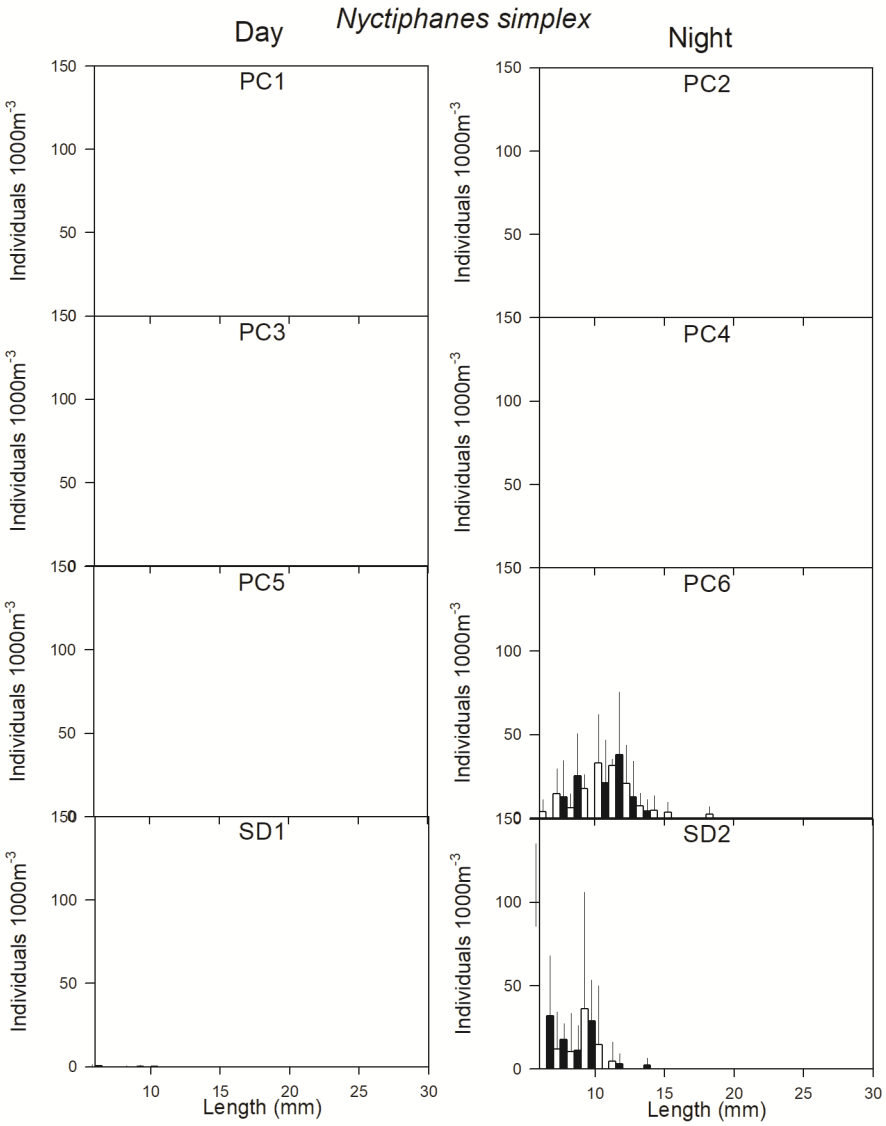

Figure S13: Mean (±95%) *Nyctiphanes simplex* abundance by length class collected by MOCNESS near Point Conception (PC) and San Diego (SD) with strobe lights on (open bars) and off (filled bars).

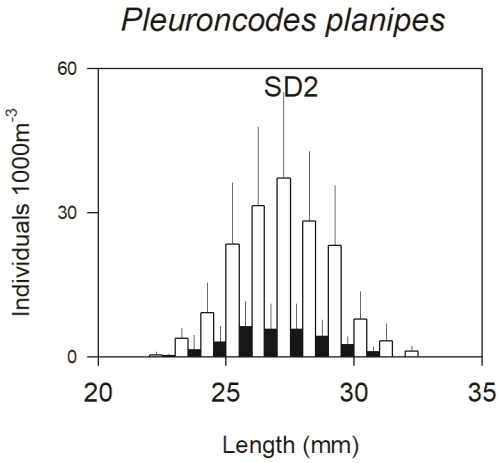

Figure S14: Mean (±95%) *Pleuroncodes planipes* abundance by length class collected by MOCNESS near San Diego (SD) with strobe lights on (open bars) and off (filled bars).